SONA COLLEGE OF TECHNOLOGY

Learning is a Celebration!

| An Autonomous Institution|

Approved by UGC | Approved by AICTE | All Eligible Programmes NBA Accredited | Ranked Institution | Affiliated to Anna University | SONA IS A SIRO

Department of
Electronics and Communication Engineering

THE INSTITUTION OF ELECTRONICS AND TELECOMMUNICATION ENGINEERS • INDIA •

IETE — THE INSTITUTION OF ELECTRONICS AND TELECOMMUNICATION ENGINEERS — सह वीर्यं करवावहै

WORLD IN SECONDS

2024 - 2025

Junction Main Road
Suramangalam (PO)
Salem-636 005. TN. India
www.sonatech.ac.in

<table>
<tr><th colspan="2">Editorial Head</th></tr>
<tr><td colspan="2">Dr.R.S.Sabeenian,
Professor &Head, Dept of ECE,
Head R&D Sona SIPRO</td></tr>
<tr><th>Staff Editorial Members</th><th>Student Editorial Members</th></tr>
<tr><td>1. Dr.G.Ravi
Professor
2. Dr.M.Jamuna Rani
Associate Professor
3. Dr.N.SasiRekha
Associate Professor
4. Prof.M.Senthil Vadivu
Assistant Professor</td><td>1. Guru Prasath R G - IV ECE
2. Thanveer Khan M-III ECE
3. Parthiv N- III ECE
4. Vijay M- IV ECE
5. Valarmathi J- IV ECE</td></tr>
<tr><td colspan="2">Magazine Co-Ordinator
Dr.K.Manju
Assistant Professor</td></tr>
</table>

PREFACE

The Communication Systems and Networks (CSN) is an inter-disciplinary group focusing on cutting-edge research in the development of reliable and efficient delivery of information for future Internet. It encompasses several areas of study including, but not limited to, telecommunication engineering, mobile communication, sensor networks, intelligent algorithms, network security and bio-inspired networks. The thrust of the research is in the development of intelligent protocols and architectures that offer seamless support for a variety of applications and user requirements in next generation networks. Work under this group includes algorithm design, protocol development and analysis, network programming, and prototype development. The main objective of the group is to establish a world-class collaborative research environment.

REVOLUTIONIZING ROAD SAFETY: AI-POWERED ROAD DEFECT DETECTION

P. SUTHARSHANA P. HARIHARAN

ABSTRACT

Road networks are necessary for cities to have convenient and safe transportation. India has an enormous network of roads, which are essential for transportation. It is critical to respond quickly to defects because they can arise from extreme events like storms and natural disasters in addition to normal wear and tear. Therefore, the need for an automated defect information gathering system that is quick, scalable, and economical arises. Using CNN model, our project "Revolutionizing Road Safety: AI-Powered Road Defect Detection for Safer Roads" seeks to transform infrastructure management and road safety. Road defects can be identified in real time. In comparison, multifunctional road inspection vehicles rely on integrated sensors, such as GPS, cameras, laser profilers, and ground-penetrating radars, enabling convenient and accurate detection of road defects. This initiative addresses the labour - intensive and error-prone nature of manual defect detection in critical infrastructure. Natural disasters further compound this issue, necessitating extensive inspections for structural integrity. The machine learning methods offers a powerful solution, allowing for the analysis of captured images to discern potential defects. The integration of convolutional neural network (CNN) architecture represents a significant advancement in the field of image processing, albeit with a notable increase in training time. A comprehensive review of ten meticulously selected research articles spanning the past decade highlights one of the most encouraging automated methods for identifying cracks, emphasizing the potential of this AI-powered system to streamline road maintenance and repair efforts while bolstering road safety in worldwide. This sophisticated system, as envisaged, leverages input images for both training and testing phases, thereby streamlining the process of identifying specific defects embedded within extensive datasets.

1 INTRODUCTION

1.1 ROAD CRACK CLASSIFICATION

The quality of roads can directly affect the development of the city. With the erosion of roads caused by rain and vehicles, various defects may appear on the road surface, such as cracks, ruts, grooves, and subsidence. The common types of pavement defects are shown in the figure below.

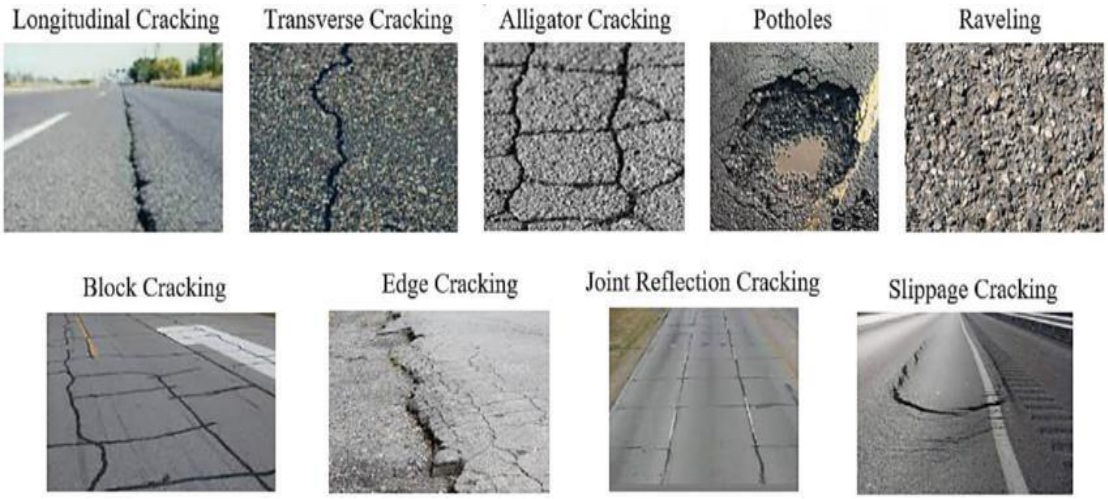

Types of road cracks

Cracks are one of the most common diseases on the pavement. It mainly has transverse cracks, longitudinal cracks, and reticular cracks. It is extremely harmful to the road surface. Especially in winter and spring, due to the infiltration of rain water, the road disease that is already in a crack state is more serious under the action of driving load. Ruts are the permanent grooves in the road surface under the repeated action of vehicle loads. This is mainly due to the unreasonable design of the asphalt mixture gradation or insufficient compaction during construction. This can make the road surface drainage poorly on rainy days, and the driving vehicle is prone to drifting and affecting the safety of high-speed driving. The grooves are mainly formed due to the lack of timely maintenance after the surface layer is cracked, which has the potential to cause a flat tire in a moving vehicle and cause a traffic accident. These defects can bring damage to the vehicles on the road. Uneven or irregular roads can lead to tire wear. Identifying road defects timely is important for pavement maintenance. Manual inspection is intuitive with the high cost and low efficiency. In order to solve this problem, various intelligent detection methods for road surface defects detection have been developed. However, there is a lack of studies summarizing the advantage and disadvantages of those intelligent detection methods. Development of Surface Cracks in PQC due to temperature difference, late joint cutting, and defective curing of PQC etc.

The cracks will allow water / mud /debris going into the cracks and widens them further. Shrinkage is another common reason for cracking. As concrete hardens and dries it shrinks. The chemical reaction, which causes concrete to go from the liquid or plastic state (or a solid state), requires water. This chemical reaction, or hydration, continues to occur for

days and weeks after you pour the concrete. Therefore, this paper conducted a comprehensive literature review on intelligent road defects detection technology. Firstly, the data collection methods of pavement defects, including cameras, ground penetrating radar (GPR), Light Detection and Ranging (LiDAR), and an inertial measurement unit (IMU), were introduced. The data processing methods, including fitting, a support vector machine (SVM), convolutional neural network (CNN), and decision tree, were then discussed. Finally, it summarized and prospected the development of road defects detection technology. Deep learning-based Object detection and localization techniques have shown immense progress in the last decade.

1.2 CONVOLUTIONAL NEURAL NETWORKS (CNN)

The CNN architecture is made up of several layers (or so-called multibuilding blocks). CNNs are the most prevalent deep learning architecture for food recognition. They consist of multiple layers of interconnected artificial neurons specifically designed to process image data. CNNs excel at learning hierarchical representations and spatial dependencies in images, making them well-suited for food recognition tasks. Each layer in the CNN architecture is described in detail below, including its function as shown in Figure

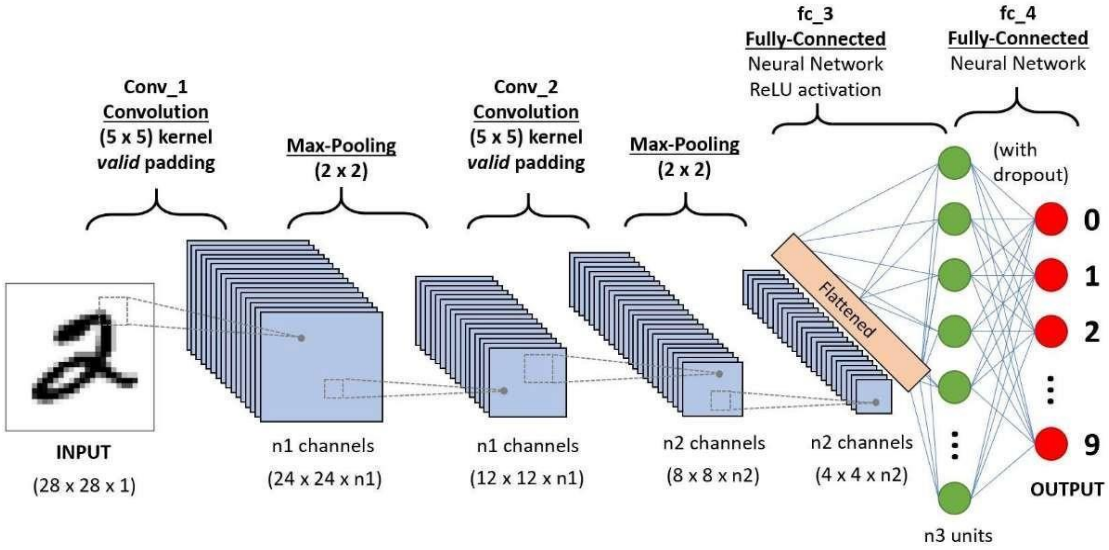

Convolutional Neural Networks

CNN (Convolutional Neural Network is a type of feed-forward artificial network where the connectivity pattern between its neurons is inspired by the organization of the animal visual cortex. Some neurons fires when exposed to vertices edges and some when shown horizontal or diagonal edges. CNN utilizes spatial correlations which exist with the

input data. Each concurrent layer of the neural network connects some input neurons. This region is called a local receptive field.

1.2.1 Convolutional Layer

The convolutional layer is the most important component in CNN architecture. It is made up of several convolutional fibers (so-called kernels). The input image is convolved with these filters to generate the output feature map, which is expressed as N-dimensional metrics. After the convolutional layer, an activation function is applied element-wise to introduce non-linearity. The most commonly used activation function in CNNs is the Rectified Linear Unit (ReLU), which sets negative values to zero and keeps positive values unchanged. The activation function enhances the network's ability to model complex relationships between the input and output. The convolutional layer computes the convolutional operation of the input images using kernel filters to extract fundamental features. The kernel filters are of the same dimension but with smaller constant parameters as compared to the input images. Asan example, for computing a 35 × 35 × 2 2D scalogram image, the acceptable filter size is f × f × 2, where f = 3, 5, 7, and so on. But the filter size needs to be smaller compared to that of the input image. The filter mask slides over the entire input image step by step and estimates the dot product between the weights of the kernel filters with the value of the input image, which results in producing a 2D activation map. CNNs mimic the human visual system but are simpler, lacking its complex feedback mechanisms and driving advances in computer vision despite these differences.

1.2.2 Activation function

ReLU is an activation function commonly used in CNNs. It introduces nonlinearity to the network by applying the function f(x)=max(0,x), which means it replaces all negative pixel values in the feature map with zero. ReLU helps the network learn complex patterns and relationships in the data. A ReLU activation function is applied after each convolution operation. This function helps the network learn non-linear relationships between the features in the image, hence making the network more robust for identifying different patterns. It also helps to mitigate the vanishing gradient problems. After the convolutional layer, an activation function is applied element-wise to introduce non-linearity. The most commonly used activation function in CNN is the Rectified Linear Unit (ReLU), which sets negative values to zero and keeps positive values unchanged. The activation function enhances the network's ability to model complex relationships between the input and output.

1.2.3 Pooling Layer

The pooling layer's primary function is to subsample the feature maps. Convolutional operations are used to generate these maps. In other words, this method condenses large-scale feature maps into smaller feature maps. At the same time, it keeps the majority of the dominant information (or features) in every stage of the pooling process. Before the pooling operation, both the stride and the kernel are size assigned in the same way as the convolutional operation. Pooling methods of various types are available for use in various pooling layers. Tree pooling, gated pooling, average pooling, min pooling, max pooling, global average pooling (GAP), and global max pooling are examples of these methods.

The most common and widely used pooling methods are max, min, and GAP Average pooling. Pooling layers provide an approach to down sampling feature maps by summarizing the presence of features in patches of the feature map. Two common pooling methods are average pooling and max pooling that summarizes the average presence of a feature and the most activated presence of a feature respectively. A limitation of the feature map output of convolutional layers is that they record the precise position of features in the input. This means that small movements in the position of the feature in the input image will result in a different feature map. This can happen with re-cropping, rotation, shifting, and other minor changes to the input image.

Two common functions used in the pooling operation are:

Average Pooling: Calculate the average value for each patch on the feature map.

Maximum Pooling (or Max Pooling): Calculate the maximum value for each patch of the feature map.

1.2.4 Fully connected layers

These layers connect every neuron in one layer to every neuron in the next layer, as seen in traditional artificial neural networks. Fully connected layers are typically placed at the end of the CNN and are responsible for combining the features extracted by the convolutional layers to perform the final classification or regression task. These layers are in the last layer of the convolutional neural network, and their inputs correspond to the flattened one-dimensional matrix generated by the last pooling layer.

ReLU activations functions are applied to them for non-linearity. Finally, a soft max prediction layer is used to generate probability values for each of the possible output labels, and the final label predicted is the one with the highest probability score.

2 PROPOSED METHODOLOGY

In this manuscript, we detail two significant contributions stemming from our innovative road defect detection system. Firstly, we introduce a method for the automation of data collection and labeling geared towards accelerometer-based classification of road defects. Prior studies in this domain, utilizing machine learning or deep learning for the identification of road defects, have consistently encountered challenges in amassing substantial datasets across diverse environments, primarily due to the complexities associated with data collection and labeling. Our solution, an automated data collection system, streamlines the acquisition and categorization of data, thereby facilitating the generation of comprehensive datasets crucial for deep learning applications.

Secondly, we propose a Convolutional Neural Network (CNN) model specifically designed to leverage this automatically collected dataset. This model is adept at identifying and distinguishing between three common road defects: speed bumps, manholes, and potholes. Through these contributions, our system not only addresses the critical challenges of data collection and labeling in the context of accelerometer-based road defect detection but also presents the potential of deep learning models to enhance the accuracy and efficiency of road defect detection. In the case of CNN approaches, detection is usually performed together with classification rather than a separate step, or a segmentation step to find crack regions or contours in the input image is often included instead of the detection step. Although CNN approaches require more computational resources than analytical or logical methods, they show improved accuracy of more than 90% through the development of new network models and continuous learning on the accumulated data. There are two main classes of object detectors that are consistently performing well on the popular Microsoft Common Objects in Context (MS COCO) dataset. In one-stage detection it is YOLO, Retina Net and in two-stage region proposal based Faster R-CNN or Mask R-CNN methods are widely used. Mask R-CNN is an extension of Faster R-CNN with an additional mask proposal branch for segmentation. YOLO has a single neural network that predicts bounding boxes and class probabilities directly from full images in one evaluation. Since the whole detection pipeline is a single network, it can be optimized end-to-end directly on detection performance. Faster R-

CNN is a region - based approaches that predicts detections based on features from a local region. This region is localized using a Region Proposal Network (RPN).

The first stage network is for region proposal on the features from convolution backbone and the second stage is a fully connected network for object classification and bounding box regression. Here the block diagram outlining the proposed methodology for detecting potholes in real-time. The process initiates with meticulous annotation of each image after compiling the dataset. The labelled data undergoes meticulous division into training and testing sets before feeding into deep learning frameworks like RCNN and SSD for individualized model training.

The weights acquired post-training play a crucial role in evaluating the model's performance on test data. The following sections will provide in-depth details of this methodology. The proposed system as shown in the figure below offers a pragmatic and cost-effective solution for data collection, relying on dashcams and devices already prevalent in most vehicles. This approach not only streamlines the process of dataset accumulation for training and testing deep learning models but also aligns with the practical constraints of research efficiency and budget. By simplifying the data collection process, our system facilitates a more robust and comprehensive exploration of road defect classification through deep learning, setting a new standard for research in this field.

Proposed approach: Block diagram demonstrating real-time pothole detection.

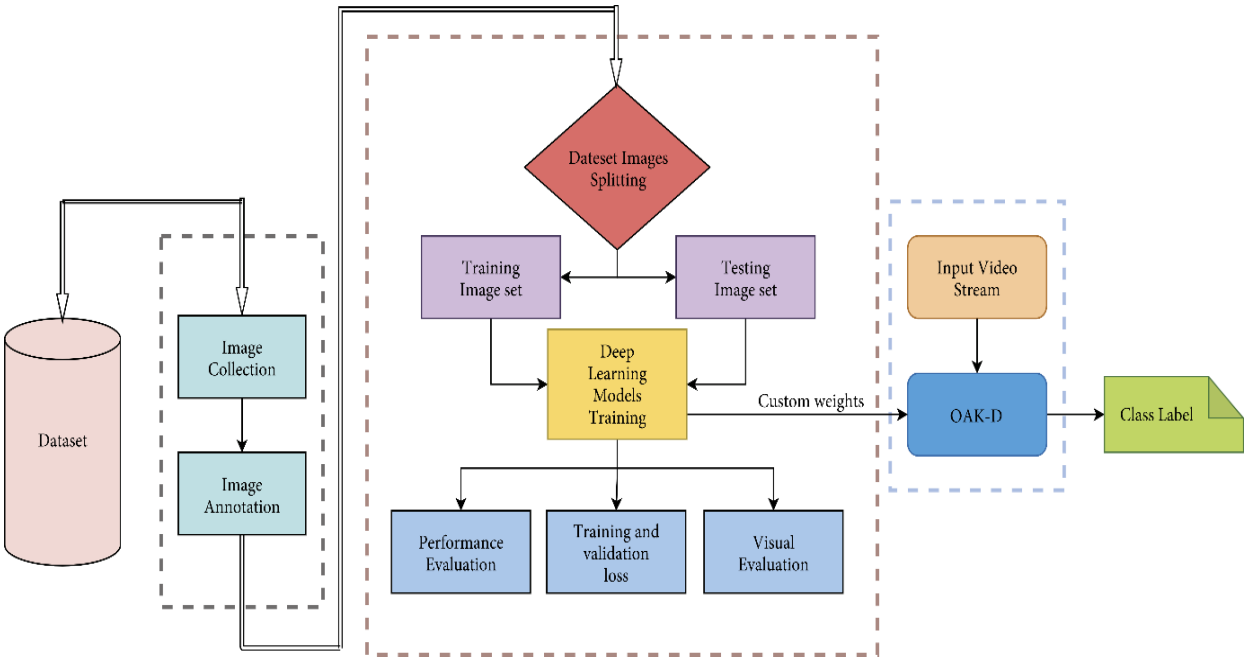

2.1 ALGORITHMS USED

2.1.1 Deep Learning Architecture

Deep learning architecture, often referred as deep neural networks, this class represents a category within machine learning models characterized by their multi-layered structure. These models can recognize intricate patterns and relationships because they are built to automatically learn hierarchical representations from data. A typical deep learning architecture comprises input and output layers, incorporating one or more concealed layers in between. Neurons within each layer are equipped with activation functions, introducing non-linearity into the network. During training, the architecture adjusts weights and biases using optimization algorithms to minimize a defined loss function. Methods like dropout and regularization are utilized to mitigate overfitting. Batch normalization stabilizes training, while the choice of output layer and activation function depends on the specific task, whether classification, regression, or other applications. There are several types of deep learning architectures, such as feedforward networks, Recurrent Neural Networks (RNNs) made for sequential data, and convolutional neural networks [16] (CNNs) made for image processing. From computer vision and natural language processing to healthcare and autonomous systems, these flexible models have shown significant success in a variety of fields. CNN Architecture:

A CNN architecture comprises two primary components:

• Using a convolutional tool, feature extraction identifies and isolates an image's distinct characteristics for analysis.

• The network for feature extraction is made up of several pairs of pooling or convolutional layers.

• Using the previously extracted features, a fully connected layer uses the convolutional process' output to determine the image's class.

• The goal of the CNN feature extraction model is to create new features that condense the existing features of an initial set, thereby reducing the volume of features in the dataset.

• Usually, the network consists of multiple CNN layers.

2.1.2 R-CNN Architecture

Since Convolution Neural Network (CNN) with a fully connected layer is not able to deal with the frequency of occurrence and multi objects. So, one way could be that we use a sliding window brute force search to select a region and apply the CNN model to that, but the problem with this approach is that the same object can be represented in an image with different sizes and different aspect ratios. While considering these factors we have a lot of region proposals and if we apply deep learning (CNN) to all those regions that would computationally very expensive. Region proposals are simply the smaller regions of the image that possibly contains the objects we are searching for in the input image. To reduce the region proposals in the R-CNN uses a greedy algorithm called selective search. Selective search is a greedy algorithm that combines smaller segmented regions to generate region proposals. This algorithm takes an image as proposal generation in that it limits the number of proposals to approximate After that these regions are warped into a single square of regions of dimension as required by the CNN model. The CNN model that we used here is a pretrained AlexNet model as shown below, which is the state-of-the-art CNN model at that time for image classification. generates region proposals on it.

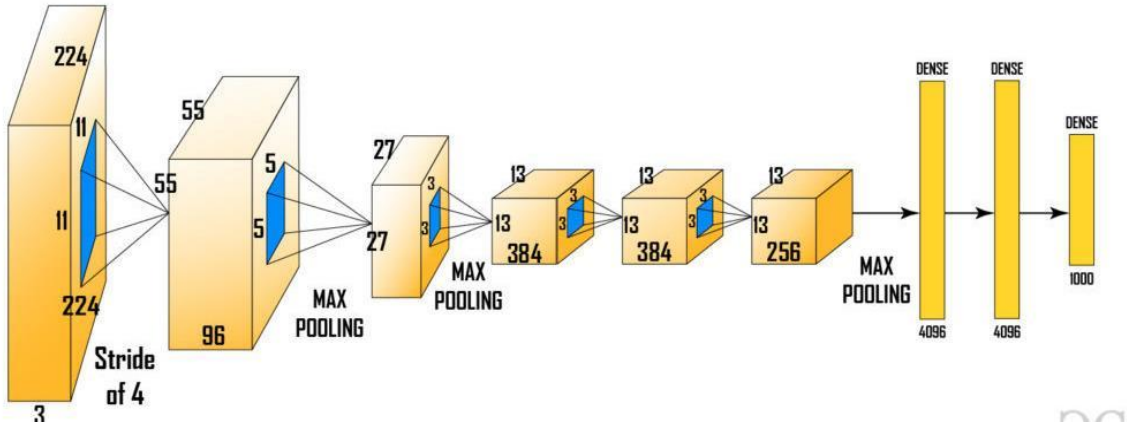

Alex Net architecture

This algorithm Convolutional Neural Network with Region-Based Approach (R-CNN) stands as a pivotal object detection framework that has made substantial contributions to the field of computer vision. Developed by Ross Girshick and his team in 2013, R-CNN marries the capabilities of Convolutional Neural Networks (CNNs) with region proposal methods to adeptly identify and pinpoint objects within images. The essence of the R-CNN architecture centers around a two-step process encompassing region proposal and feature extraction. In the initial phase, a set of region proposals takes shape through techniques like

selective search. These proposals represent prospective bounding boxes that are deemed probable receptacles for objects of interest. The diversity and quality of these region proposals hold critical significance in shaping the overall efficacy of R-CNN. Subsequently, the second stage delves into feature extraction, where each region proposal undergoes individual transformation to a standardized size, often set at 224x224 pixels. These transformed regions are then channelled through a pre-trained CNN model, such as AlexNet or VGG-16. The CNN model has previously undergone fine-tuning on an expansive dataset, such as ImageNet, to acquire generalized feature extraction capabilities. Consequently, this process yields a unique feature vector for every region proposal, encapsulating the visual information enclosed within that specific region.

Post feature extraction, R-CNN engages an ensemble of Support Vector Machine (SVM) classifiers, one for each object category of interest. These classifiers are meticulously trained to distinguish between two categories: positive (indicating the presence of the object) and negative (indicating the absence of the object) samples. This classification step serves as the decision making phase, providing insights into whether a particular category of object is present within the given region proposal. Moreover, R-CNN incorporates a bounding box regression component.

This component's role revolves around refining the coordinates of the region proposal's bounding boxes. To accomplish this, a linear regression model is harnessed to predict the necessary adjustments for aligning the bounding box accurately with the object within the region proposal. The process of reducing redundant predictions involves applying a technique known as non-maximum suppression to the bounding box predictions. This step is pivotal in eliminating redundancy and handling overlapping detections, ensuring that only the most confident detection results are retained when multiple bounding boxes overlap significantly.

2.1.3 SVM (Support Vector Machine)

The feature vector generated by CNN is then consumed by the binary SVM which is trained on each class independently. This SVM model takes the feature vector generated in previous CNN architecture and outputs a confidence score of the presence of an object in that region. However, there is an issue with training with SVM is that we required AlexNet feature vectors for training the SVM class. So, we could not train AlexNet and SVM

independently in paralleled manner. This challenge is resolved in future versions of R-CNN (Fast RCNN, Faster R-CNN, etc.).

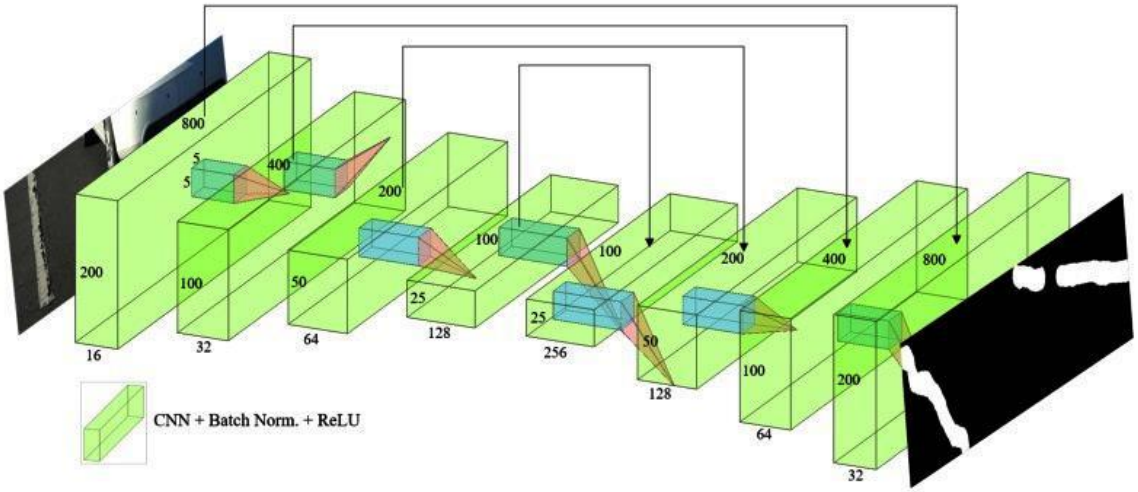

CNN architecture for road surface damage detection technique

2.1.4 Faster RCNN

In the field of computer vision, Faster R-CNN, an advancement of the original R-CNN (Region-Based Convolutional Neural Network), signifies a notable breakthrough in object detection. This architecture was introduced by Shaoqing Ren, et al., in 2015, and it addresses several limitations of its predecessor, providing an efficient and highly accurate solution for object detection tasks. The region proposal networks (RPNs) concept is the foundation of Faster R-CNN Rather than depending on external region proposal techniques such as selective search, Faster R-CNN directly incorporates an RPN into the network itself. This RPN shares convolutional layers with the subsequent object detection network and learns to generate region proposals, streamlining the process and significantly improving efficiency.

The Region Proposal Network (RPN) and the Fast R-CNN network are the two main parts of the architecture. After scanning the input image, the Region Proposal Network generates a set of region proposals, each of which is connected to a region of interest (RoI). These suggestions function as possible locations for the objects. The Fast R-CNN network is in charge of categorizing and honing these region suggestions into accurate object detections concurrently.

The effective feature extraction capabilities of a pre-trained CNN model, usually VGG-16 or Res Net, are retained by Faster R-CNN. These networks extract high-level

features from the input image, which the RPN and the Fast R-CNN components use together. These characteristics are essential for performing object classification as well as generating precise region proposals.

Anchor boxes are predefined bounding boxes with a range of sizes and aspect ratios that make up the Region Proposal Network. These anchor boxes are evaluated by the RPN, which then modifies them to line up with appropriate objects. After that, it rates each proposal to ascertain how likely it is to contain an object and then refines it to increase the accuracy of localization.

The region proposals produced by the RPN are fed into the Fast R-CNN network via a RoI pooling layer, which aligns and resizes each proposal to a fixed size so that it can be used with the fully connected layers. Following that, a series of fully connected layers and related soft max classifiers are applied to these proposals in order to classify objects into predefined categories using Faster R-CNN.

2.2 Data Collection

We gathered a training dataset using cameras installed on a vehicle while driving on roads to teach a neural network model to detect road surface damage automatically. The images were captured at a resolution of 1920 × 1080, placed strategically in areas with high transportation activity. This dataset considers only four damage categories, comprising majorly of cracks and potholes, namely D00, D10, D20, and D40.

2.2.1 Road Damage Dataset

Gather a dataset of road images with annotations indicating the presence and location of various types of road damage, including potholes. Split the dataset into training, validation, and test sets. Ensure that the distribution of different types of road damages is representative in each set. The latest dataset is collected from India and in addition to other foreign was made available by GIS

As we fine tune the models, we need to create composite datasets with Train + Test (T+T) and Train + Val (T+V) dataset composition. This will help model use entire data for learning and evaluation. Verifying the performance of a model in any classification task, including the classification of road defects using the ResNet architecture, involves the critical step of analyzing the confusion matrix and calculating various performance parameters. The

confusion matrix is a powerful tool that provides insights into a model's ability to correctly classify instances. There are four main parts to the confusion matrix.

When the model predicts the positive class with accuracy, it is called True Positive (TP).True Negative (TN): These are instances in which the model predicted the negative class with accuracy. False Positive (FP): These are instances of false alarms where the model predicts the positive class when the actual class is negative. False Negative (FN): The model tends to miss the opportunities for accurate classification when it incorrectly predicts the negative class when the actual class is positive.

Performance Matrix Formulae

S. No.	Performance Metrics	Formula
I.	precision	$tp\ /tp + fp$
II.	recall	$tp/tp + fp$
III.	F1 score	$2 * (precision * recal\ precision + recall)$
IV.	accuracy	$tp + tn/tp + tn + fp + fn$

2.2.2 Metrics

• IoU (Intersection over union): IoU measures the overlap between 2 boundaries. We use that to measure how much our predicted boundary overlaps with the ground truth (the real object boundary). In some datasets, we predefined an IoU threshold (say 0.5) in classifying whether the prediction is a true positive or a false positive.

• Mean Average Precision (mAP)**:** In order to calculate mAP in the context of Object Detection, we first compute the Average Precision (AP) for each class, and then compute the mean across all classes. Given True positive = Number_of_detection with IoU > 0.5

2.2.3 Creating the Training DB

We collected training datasets through cameras and large datasets from Kaggle to train and test. As shown in the figure, the part of the input image with road surface damage appears as green box, which identify the specific part of damaged road. Figure 5.2.3 shows trained labelled image examples to detect road surface damage which shows potholes of damaged roads.

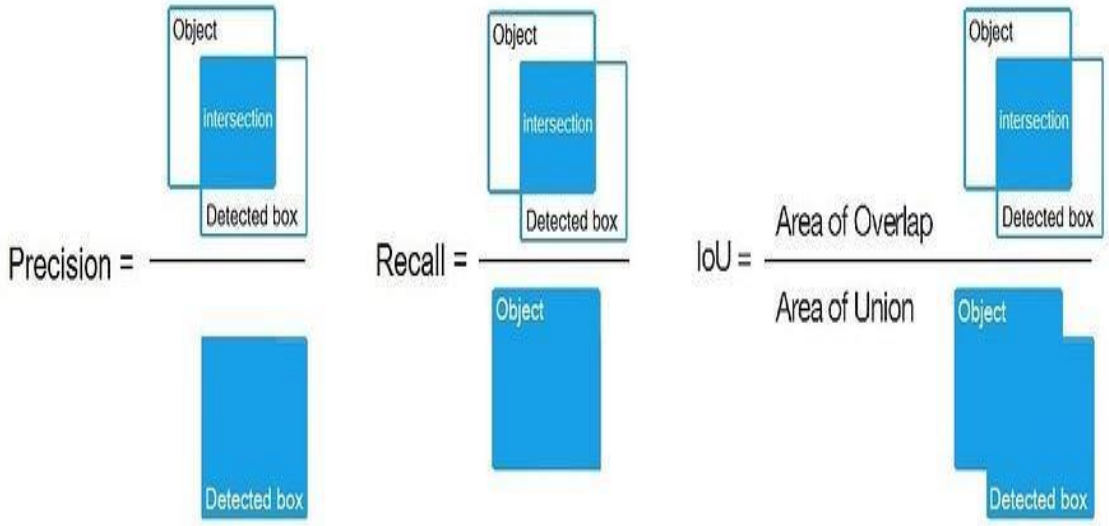

Precision, Recall, IoU

2.3 DATA ANNOTATION TOOLS

Data annotation tools are essential for labeling and annotating data for training machine learning models. For the project of deciphering Ancient Tamil stone inscriptions using deep learning techniques, data annotation tools are essential for labeling and annotating images to train machine learning models effectively. Here are some data annotation tools suitable for this project:

Creating the Training images

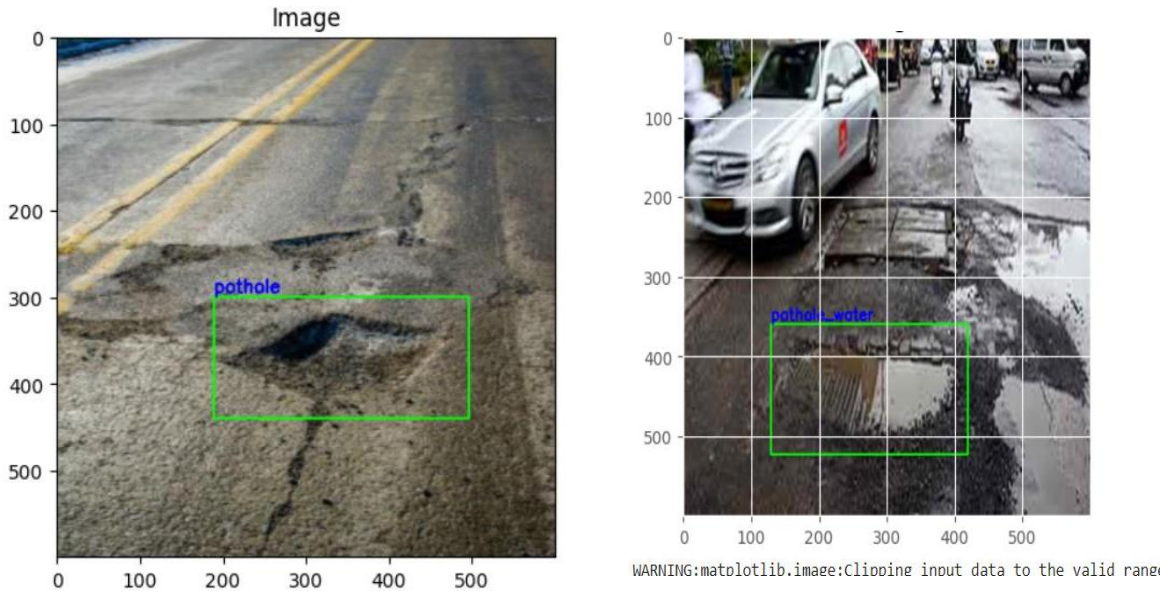

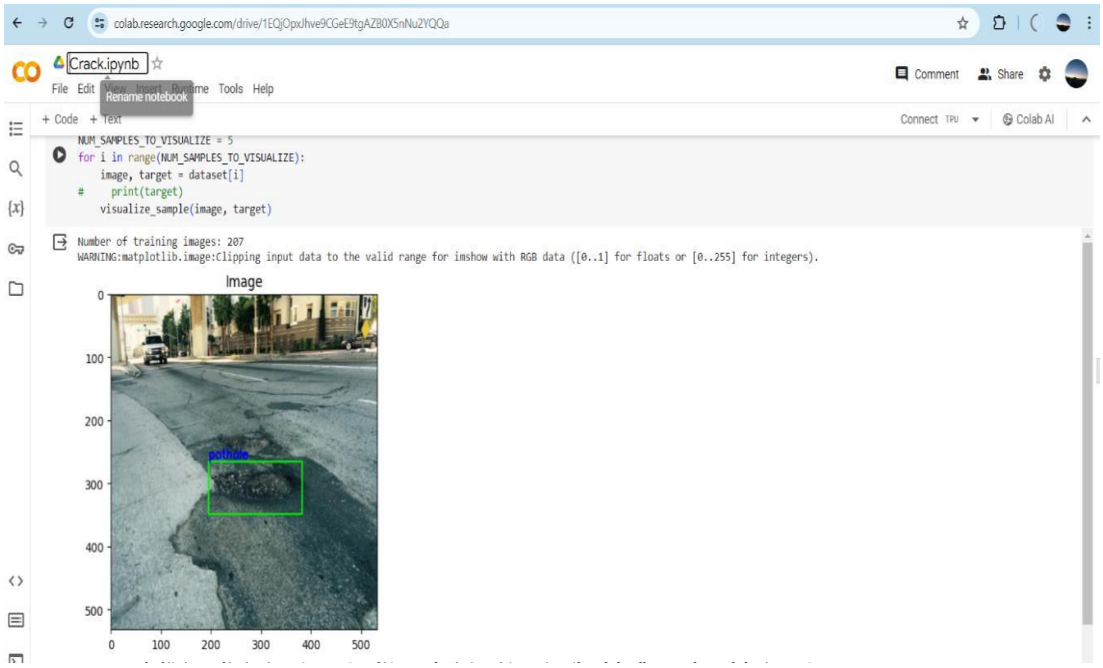

- Labelling drawing bounding boxes around things of interest in photos is possible with Labelling, an open-source image annotation tool. It may be used with a variety of deep learning frameworks because it supports multiple annotation formats, including Pascal VOC and YOLO.
- VGG Image Annotator (VIA) VIA is a web-based annotation tool that enables users to annotate images with polygons, rectangles, or circles. It supports multiple annotations per image and provides options for exporting annotations in various formats.
- COCO Annotator COCO Annotator is a simple and intuitive tool for annotating images with bounding boxes and segmentation masks. It is designed specifically for creating annotations in the COCO format, which is widely used in object detection tasks.
- Amazon Sage Maker Ground Truth High-quality annotations for machine learning model training are provided by the completely managed data labeling service Amazon Sage Maker Ground Truth. It works with labeling workflows that are both automatic and human-in-the-loop, and it easily connects with other AWS services.
- Data turks Data turks is a lightweight annotation tool that supports annotation formats such as bounding boxes, polygons, and key points. It offers an intuitive user interface and easy integration with machine learning pipelines

Test 1 and Test 2 data is provided by the challenge committee for evaluation and submission. Upon submission an Average F1 score is added to the private leaderboard as well as a public leaderboard if it exceeds all the previous scores in our private leaderboard.

Sample of marked, damaged, vehicle images from the dataset.

2.3.1 Evaluation Strategy

Evaluation strategy includes matching of the predicted class label for the ground truth bounding box and that the predicted bounding box has over 50% Intersection over Union (IoU) in area. Precision and recall are both based on evaluating Intersection over Union (IoU), which is defined as the ratio of the area overlap between predicted and ground-truth bounding boxes by the area of their union. The evaluation of the match is done using the Mean F1 Score metric. The F1 score, commonly used in information retrieval, measures accuracy using the statistics of precision p and recall r. Precision is the ratio of true positives (tp) to all predicted positives ($tp + fp$) while recall is the ratio of true positives to all actual positives (tp + fn). Maximizing the F1 -score ensures reasonably high precision and recall. The F1 score is given by:

$$F_1 = 2 \times \frac{\mathrm{p} \times \mathrm{r}}{\mathrm{p} + \mathrm{r}} \; where \; \mathrm{p} = \frac{\mathrm{tp}}{\mathrm{tp} + \mathrm{fp}} \; and \; \mathrm{r} = \frac{\mathrm{tp}}{\mathrm{tp} + \mathrm{fn}}$$

Avg F1 score serves as a balanced metric for precision and recall. This is the metric we obtain in our private leaderboard, upon submitting the evaluation results on Test 1 or Test 2 datasets.

3 WORKING OF THE SYSTEM

The working of a system for road damage detection, such as one employing a Convolutional Neural Network (CNN) like Res Net, involves several steps. First The system functions by gathering real-time data from an array of vehicle mounted sensors, including cameras. This data is then processed and amalgamated to construct a comprehensive depiction of the road conditions and the vehicle's behaviour. At the system's core lies an AI model, typically a CNN model, which has undergone training to scrutinize the data and spot road defects like cracks and potholes. Upon detecting a defect, the system triggers a response mechanism that can alert the driver, notify a central monitoring centre, or inform road maintenance authorities. The vehicle is equipped with a user-friendly interface that offers real time information on road conditions and detected defects. Concurrently, data is stored for historical analysis, supporting future maintenance planning.

The system rigorously complies with regulatory standards and undergoes routine maintenance and updates to ensure secure and effective operation. By leveraging data and AI, it equips both drivers and authorities with indispensable insights, leading to a transformative enhancement in road safety and more efficient road maintenance practices. The data collected from the raw data collection step are pre-processed to generate deep learning analyses. The data preprocessing step first extracts the raw data collected to identify segments indicative of road defects. This is achieved through a threshold-based classification technique, where significant fluctuations in acceleration sensor readings suggest potential road defects. The threshold values used for this determination are established through experimental methods. If the acceleration value of the raw data exceeds the threshold, both the acceleration values and dashcam video segments are trimmed to lengths that contain road defect information. This trimming, or “data slicing”, leverages the temporal data captured by the acceleration sensors and dashcam footage to ensure precise segmentation. The extent of each data slice is calculated based on the vehicle’s speed and the estimated length of the road defect, aiming to cover the entire duration a vehicle traverses a defect.

$L\ slice = L\ defects / S\ min$ =3.6 m/0.277 m/s =2.60869 s ≅3 s

Utilizing the maximum known speed bump length of 3.6 m [**39**] and a minimal vehicle speed of 5 km/h (or 0.277 m/s), the slicing length is determined to be approximately 3 s to accommodate the defect passage duration.

3.1 PRE-PROCESSING

We looked at segmentation as a way to eliminate background and noise from the image so that we can analyse features only on the road. A PyTorch and Detection based Deep Lab V3+ implementation is used for segmentation contours and image cropping.

1. Input Data Acquisition: The system begins by acquiring input data, typically in the form of images or videos, captured by cameras mounted on vehicles or drones. These images contain visual information about the road surface.

2. Preprocessing: Before feeding the data into the CNN model, pre-processing steps may be applied. This can include resizing the images to a standard size, normalizing pixel values, and possibly augmenting the dataset through techniques like rotation, flipping, or adjusting brightness and contrast. Preprocessing aims to standardize and enhance the data for better model performance.

The dataset used to train a single Faster R-CNN model.

Model	Hyper-Parameters	Pre-Processing	Avg F1(Test 1)
Faster RCNN 27k, Resnet 50	Batch 128, LR 0.005	Segmentation	0.4872
		None	0.4945

Segmentation Benefit

The CNN learns hierarchical representations of the input images, gradually extracting features that are increasingly abstract and meaningful for the task of road damage detection.

Feature Extraction: The CNN learns hierarchical representations of the input images, gradually extracting features that are increasingly abstract and meaningful for the task of road damage detection. Lower layers may detect simple features like edges and textures, while higher layers may capture more complex patterns indicative of road damage.

Classification/Segmentation: Depending on the specific task, the CNN outputs predictions in one of two ways:

Classification: The CNN predicts the presence or absence of road damage, including potholes, in the input images. This is typically a binary classification task where the model assigns a probability score to each class (e.g., damaged vs. undamaged).

Segmentation: The CNN produces pixel-wise segmentation masks, indicating the location and extent of road damage in the input images. Thesis more detailed and provides fine-grained information about the exact areas of damage.

Output Visualization/Reporting: The system generates output visualizations or reports based on the model predictions. This could involve overlaying detected road damage regions on the original images, generating damage severity maps, or providing summary statistics about the detected damage instances.

Feedback and Iteration: The system may incorporate feedback mechanisms to continuously improve its performance. This could involve collecting ground truth labels for detected road damages, retraining the model with additional data, finetuning hyperparameters, or updating the model architecture based on performance metrics and user feedback.

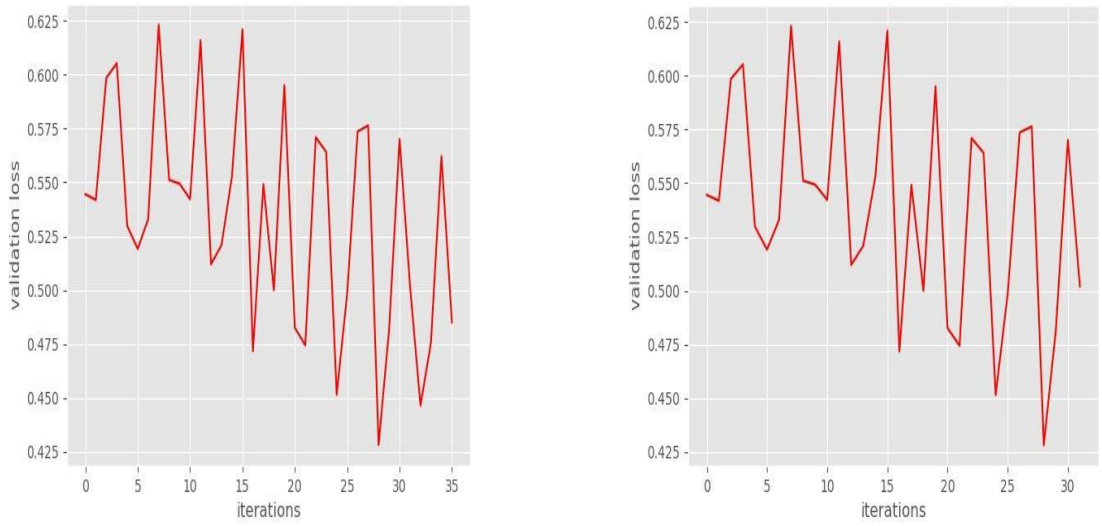

Feedback and Iteration

Overall, the system's working revolves around leveraging CNN-based algorithms to analyze input images, extract meaningful features, and make predictions or segmentations related to road damage, with the ultimate goal of aiding in infrastructure maintenance and ensuring road safety.

3.2 Post processing

In this step we look at operations after detection. The resulting bounding boxes are filtered at 0.7 confidence threshold. Additionally, the detections are sorted by confidence and

only the top 5 bounding boxes are sampled for best submission. In road damage detection using a CNN like ResNet-50, postprocessing plays a crucial role in refining the output generated by the model. Here are post-processing techniques used specifically in used in our project and its explanation.

Thresholding is a simple yet effective technique used to binarize segmentation masks produced by the CNN. It involves setting a threshold value, above which pixel values are considered as road damage, and below which they are considered background. This helps in separating the damaged areas from the rest of the road surface.

```
]

# define the detection threshold...
# ... any detection having score below this will be discarded
detection_threshold = 0.5
```

```
['../input/pothole-model/test_data/potholes85.png', '../input/pothole-model/test_data/potholes36.png', '../input/pothole-model/te
st_data/potholes8.png', '../input/pothole-model/test_data/potholes12.png', '../input/pothole-model/test_data/potholes21.png',
'../input/pothole-model/test_data/potholes84.png', '../input/pothole-model/test_data/potholes37.png', '../input/pothole-model/tes
t_data/potholes39.png', '../input/pothole-model/test_data/potholes91.png', '../input/pothole-model/test_data/potholes13.png',
'../input/pothole-model/test_data/potholes32.png', '../input/pothole-model/test_data/potholes0.png', '../input/pothole-model/test
_data/potholes73.png', '../input/pothole-model/test_data/potholes10.png', '../input/pothole-model/test_data/potholes68.png']
Test instances: 15
```

Test Instances

Morphological operations such as dilation and erosion are often applied to the binary segmentation masks to smooth out the boundaries of detected road damages and fill in small gaps or holes. Dilation expands the regions of road damage, while erosion shrinks them. By applying these operations iteratively, the segmentation masks can be refined to better match the actual shapes of the damages.

Connected component analysis is used to identify and label distinct regions or objects in the binary segmentation masks. It helps in separating individual instances of road damage from each other and from other background elements. This information can be used to compute statistics about the size, shape, and spatial distribution of detected damages.

Filtering based on Size and Shape - After connected component analysis, filtering can be performed to remove small or spurious regions detected as road damage. This is typically done by setting a minimum threshold on the area or perimeter of the connected components.

Additionally, shape-based filters can be applied to exclude regions that do not resemble typical road damages, such as long narrow streaks or isolated dots.

Smoothing and Refinement - Techniques such as Gaussian smoothing or median filtering may be applied to the segmentation masks to further refine them and remove noise or irregularities. These filters help in producing more visually appealing and consistent results, improving the interpretability of the detected road damages.

Overlap Resolution - In cases where multiple instances of road damage overlap with each other or with the background, additional processing may be needed to resolve these overlaps. This could involve prioritizing larger or more significant damages, or using clustering algorithms to group closely located damages into coherent clusters. By incorporating these post-processing techniques into the road damage detection pipeline, the output generated by the CNN model can be refined and enhanced, leading to more accurate and reliable identification of road damages such as potholes, cracks, and surface defects.

3.3 SOFTWARE REQUIRED

Python: Python is the de facto language for machine learning and offers a rich ecosystem of libraries for data manipulation, visualization, and modelling.

Anaconda: Anaconda is a distribution of Python that comes with many data science libraries pre-installed. Miniconda is a lightweight version that allows you to install only the packages you need.

Deep Learning Frameworks: Choose one of the popular deep learning frameworks that support CNNs:

Tensor Flow: Developed by Google, TensorFlow offers high-level APIs for easy model building and deployment.

PyTorch: Developed by Facebook, PyTorch is known for its dynamic computation graph, making it flexible for research and development.

Keras: Keras is a high-level neural networks API, written in Python and capable of running on top of TensorFlow, Theano, or Microsoft Cognitive Toolkit (CNTK).

Jupyter Notebook: Jupyter Notebooks provide an interactive environment for running Python code, visualizing data, and explaining your workflow. It's widely used for experimentation and prototyping in machine learning.

Once you have these tools installed, you can start building and training CNN models for various machine learning tasks such as image classification, object detection, and image segmentation.

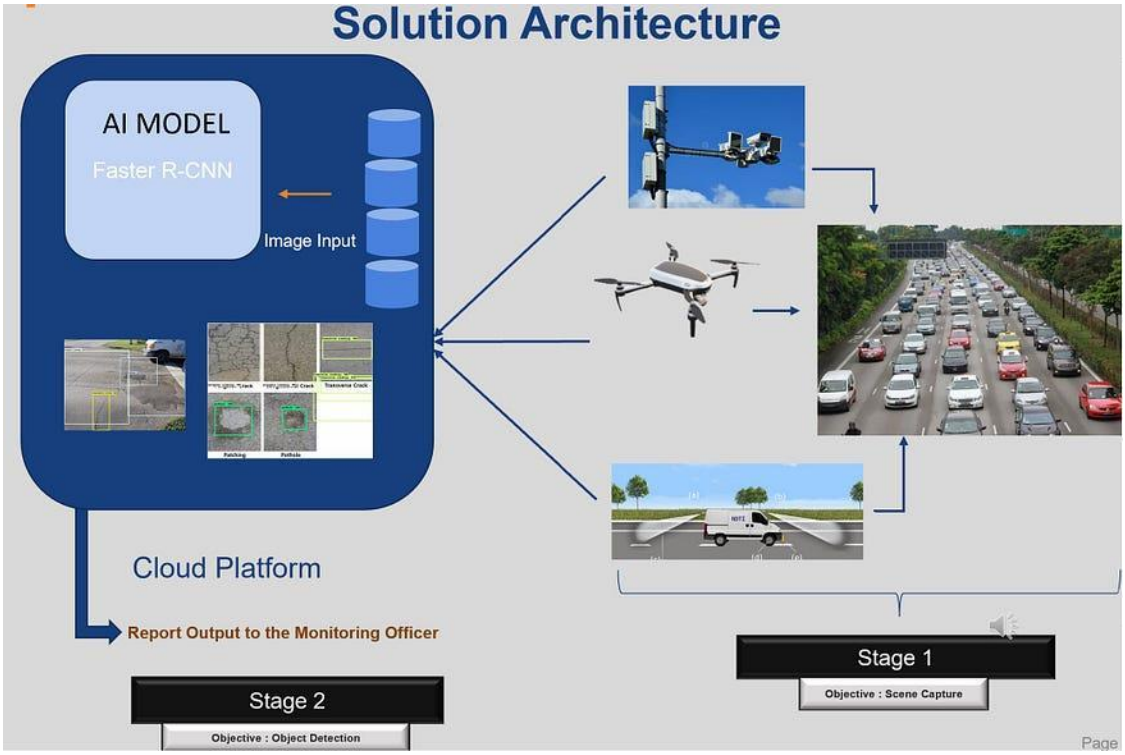

Sample Architecture represent where this model used on a commercial basis

The architecture presents a two-stage monitoring process. In the first stage, a lightweight process is employed to capture the target scenes, and the data is then transferred to the second stage. Stage 1 can be implemented using either a drone or a stationary CCTV [camera. This initial stage is connected to a high performance cloud infrastructure where the second stage is situated. In stage 2, the model discussed in this blog (Faster R-CNN) can be hosted to achieve higher precision predictions and generate corresponding feedback based on the predictions.

4 RESULTS AND DISCUSSION

The evaluation of the trained model's performance was gauged using three key metrics: Precision, Recall, and F1-score. Precision represents the proportion of accurately predicted features (true positives) relative to the total number of predicted features (true positives and false positives). It highlights the precision of the model in identifying relevant features. On the other hand, Recall signifies the percentage of accurately predicted features in comparison to the total number of features belonging to the actual class (true positives and

false negatives). It provides insights into the model's ability to capture all relevant features within a given class.

The implementation leverages a pre-trained Faster R-CNN model with a ResNet-50 backbone, showcasing the efficacy of transfer learning in adapting the model to the task of road damage detection. The resulting detection outputs are visualized with bounding boxes encapsulating the identified potholes and areas with pothole water, offering a clear visual representation of regions requiring attention or repair. The incorporation of bounding boxes in the output offers a pragmatic approach to visualize both the scope and whereabouts of road damage.

This visual depiction assists maintenance teams and decision-makers in comprehending the spatial distribution of concerns, enabling a focused and effective strategy for deploying repair initiatives. Moreover, the system's precision in identifying potholes and discerning water within them contributes to a more accurate damage assessment, minimizing the likelihood of oversight in crucial maintenance zones. This output functions as a valuable tool for road maintenance and monitoring, providing a rapid and automated approach to assess the condition of road surfaces. The application of such technologies holds the potential to enhance the efficiency of road maintenance efforts, contributing to overall road safety and infrastructure management.

Concerning scalability, the approach demonstrates its ability to adapt to a wide range of road environments and various levels of damage. This versatility positions the system as a flexible solution suitable for diverse geographic locations and varying road conditions. The incorporation of deep learning techniques guarantees the model's capability to generalize effectively to novel datasets, establishing its robustness in tackling challenges arising from evolving road damage scenarios.

As for now, it provides average performance across different object classes in the VOC PASCAL dataset. The output presented effectively demonstrates the detection of both potholes and pothole water in a road image. Through the utilization of advanced computer vision and deep learning techniques, the system accurately identifies and delineates areas of road damage, precisely locating instances of potholes and indicating the presence of water within these damaged areas.

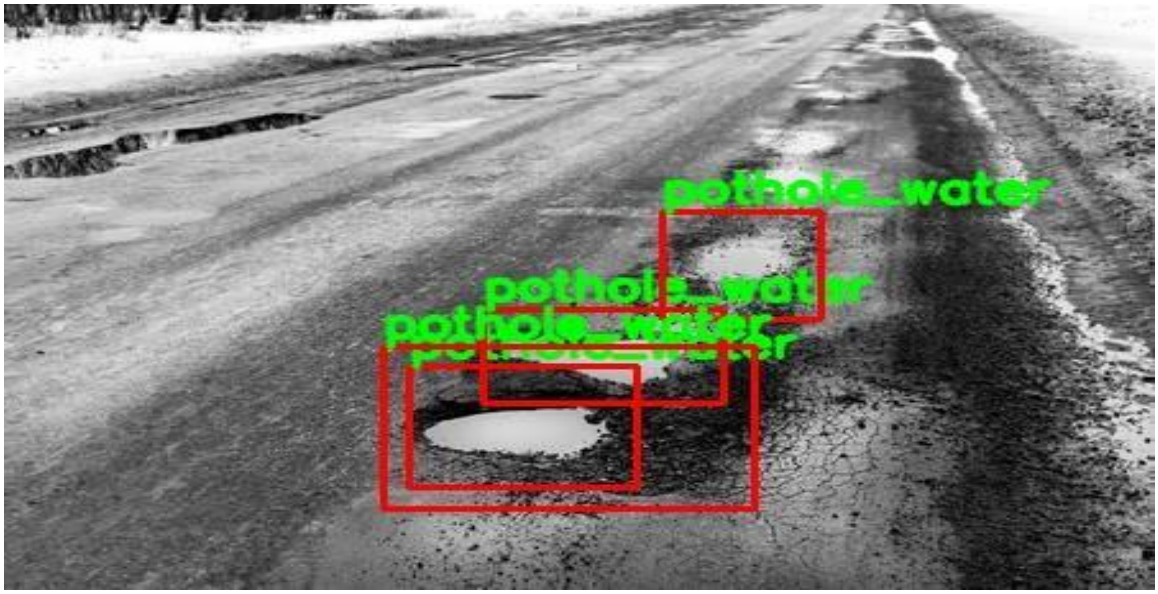

Identifying Potholes and Pothole Water Damage in Road Images

The detection process employs sophisticated algorithms that have been trained to recognize specific visual patterns associated with road damage.

4.1 Graphs:

Graphs can be instrumental in various stages of the road crack detection process. Visualizing graphs such as histograms or bar charts can help you analyze the distribution of images with and without cracks. This insight is crucial for ensuring that your dataset is balanced and representative, which is essential for training an effective model. During model training, monitoring the loss and accuracy metrics over epochs through graphs can provide valuable feedback on the model's learning progress. Plots showing the training and validation loss can help you identify whether the model is overfitting or underfitting. By observing these

trends, you can make informed decisions about adjusting hyperparameters or stopping training early to prevent overfitting. After training model, visualizing evaluation metrics such as precision, recall, and F1-score through graphs can give you a comprehensive understanding of its performance. Receiver Operating Characteristic (ROC) curves and Precision-Recall curves are particularly useful for binary classification tasks like crack detection. These graphs allow you to analyze the trade-off between true positive rate and false positive rate or precision and recall, respectively, at different threshold values. Once model is deployed, you can use graphs to visualize its predictions on new road images. Overlaying the detected cracks on the original images using bounding boxes or segmentation masks can provide valuable insights into the model's performance in real-world scenarios.

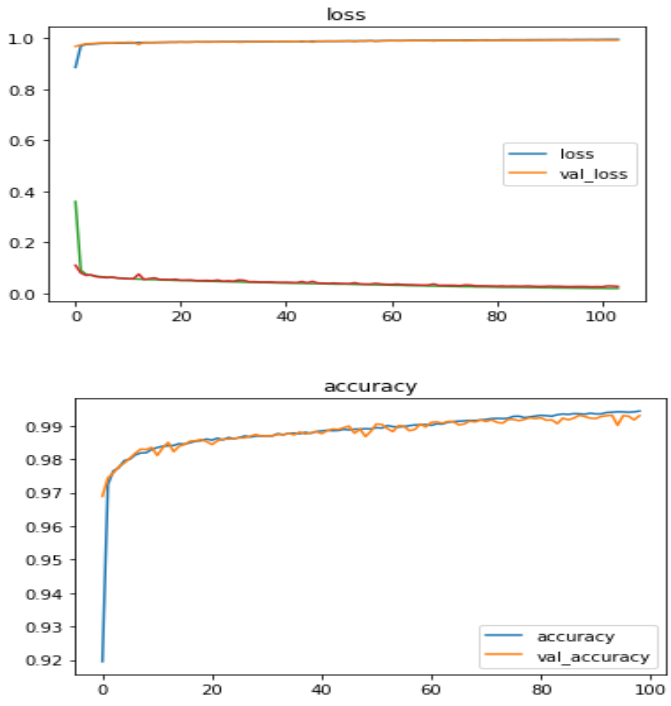

Training and validation loss

This visualization helps stakeholders, such as road maintenance authorities, understand where cracks are detected and assess the model's effectiveness in identifying different types of cracks. If we experiment with multiple models or variations of the same model architecture, comparing their performance using graphs can aid in decision-making. You can create side-by-side plots of evaluation metrics or detection visualizations to determine which model performs best for your specific requirements.

IMPLEMENTATION OF BATTERY DEGRADATION ON LITHIUM-ION BATTERIES USING PYNQ-FPGA

GIRISHANKAR R RAGHUL G

ABSTRACT

Predicting the remaining usable life (RUL) of a lithium-ion battery properly is vital for appropriate maintenance and overall health evaluation, which is particularly pertinent in the burgeoning electric vehicle industry, where optimising battery performance, is essential. Determining the rate of battery deterioration is a complex task because of the wide variety of internal and external elements that could affect it. Our study addresses this challenge by using datasets on battery ageing sourced from NASA's Prognostic Centre of Excellence (PCoE) to introduce a data-driven approach for State of Health (SOH) estimation. In our pursuit of RUL prediction, we have devised a machine-learning model employing the ADAM optimiser for optimisation. Consequently, our proposed model utilises software programming on PYNQ FPGA to discern battery degradation. The findings of these innovative approaches are thoroughly analysed and assessed, showcasing the effectiveness of our approach in navigating the complexities associated with predicting battery RUL.

1 INTRODUCTION

Using fossil fuels has given rise to adverse environmental consequences, including air pollution and global warming, leading to heightened health issues and socio-economic impacts on a global scale. Because of the severity of the problems in using fossil fuels, many nations are entering international agreements and implementing domestic policies to address and mitigate the environmental impact of fossil fuel usage. As a result, there is a growing emphasis on prioritizing renewable energy production worldwide, with a particular focus on photovoltaics (PV) and wind energy.

Although wind and photo voltaic are commonly perceived as non-dispatchable and have minimal impact on grid stability, it is crucial to incorporate batteries and energy storage technologies. Batteries made with lithium have rapidly become the industry standard due to their extended cycle life, excellent power efficiency, and minimal energy consumption. The increased attention on electric vehicles (EVs) powered by lithium batteries is notable, driven by the desire to address the limitations of fossil fuels. To promote the adoption of EVs, the Indian central government has implemented several promotional measures over the past

decade. These measures include tax incentives for EV owners and the development of public EV charging infrastructure.

Rechargeable Lithium-ion (Li-ion) batteries are crucial components in numerous electronic devices due to their lightweight design, high efficiency, long-lasting performance, and impressive energy storage capabilities. However, the capacity of Li-ion batteries tends to decrease with more charge-discharge cycles. The forecast for Remaining Useful Life (RUL) is becoming increasingly significant in the field of Prognostics and Health Management (PHM) as it strives to ensure the dependability and safety of electronic equipment. Predicting RUL in advance provides crucial information for maintenance and replacement decisions, contributing to overall safety. Fig. 1 depicts a toy example illustrating the usage pattern of a battery.

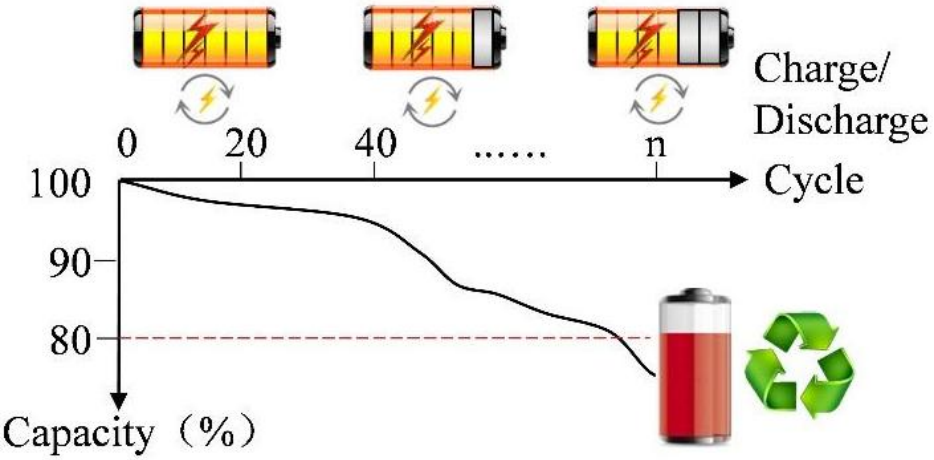

Capacity degradation over cycles

This project offers greater efficiency and customization potential by enabling the design of specialized hardware architectures of FPGA. Python plays a pivotal role in this project. Building a deep learning model to detect capacity decline facilitates access to datasets. Python also makes building a user-friendly GUI easier and integrates the system with the FPGA board. This versatile language ensures the efficient operation and optimization of the FPGA-based SoH prediction system, enabling comprehensive and effective battery management solutions.

Implementing battery degradation on lithium-ion batteries using PYNQFPGA involves integrating hardware and software components to model and analyze the degradation process effectively. PYNQ (Python Productivity for Zynq) is an open-source

project that enables programming Zynq devices with Python and using the capabilities of programmable logic and microprocessors within a single system.

Lithium-ion batteries are crucial components in various applications, including electric vehicles and renewable energy storage systems. However, they suffer from degradation over time, which affects their performance and lifespan. By implementing battery degradation on PYNQ-FPGA, researchers and engineers can simulate and analyze degradation mechanisms in real-time, allowing for better understanding and optimization of battery management strategies. Creating mathematical models or algorithms to simulate battery degradation phenomena such as capacity fade, impedance growth, and voltage decline over cycles or time. Utilizing FPGA resources to accelerate the computation-intensive tasks involved in battery degradation modelling. This may include designing custom hardware accelerators or utilizing existing IP cores for signal processing and data analysis. Developing Python-based software interfaces to interact with the FPGA accelerated degradation model. PYNQ provides a convenient framework for integrating custom FPGA designs with Python scripts, enabling rapid prototyping and experimentation. Validating the accuracy of the degradation model using experimental data and optimizing the model parameters for better predictive performance. This iterative process helps refine the model and improve its reliability in real-world applications. Overall, implementing battery degradation on PYNQ-FPGA offers a flexible and efficient platform for studying and mitigating the effects of degradation in lithium-ion batteries, ultimately leading to improved battery management strategies and enhanced reliability in various applications.

2 PROPOSED METHOD

2.1 INTRODUCTION

A sophisticated AI-based battery management system (BMS) can estimate a lithium-ion battery's precise health status by utilizing long-term memory (LSTM) technology. The system, synthesized on the Xilinx Zynq SoC PYNQ Z2 board and implemented in Python, achieves impressive results with low RMSE values during validation and training.

The dataset includes charging and discharging cycles, temperature, voltage, and current information. The Random Forest Regressor enhanced the model due to its expertise in handling complex data connections. Through training, the model acquired the ability to make accurate predictions on new data by recognising patterns from previous data, enabling it to generalise effectively.

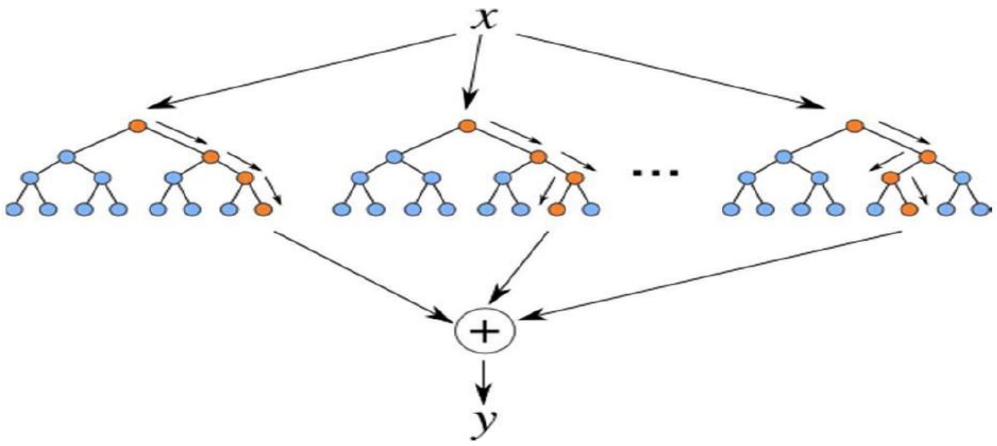

Random Forest Regressor

The Random Forest Regressor enhanced the model due toits expertise in handling complex data connections. Figure 2 illustrates the architecture of the model. It underwent meticulous configuration with hyper parameters tailored for optimal performance. Through training, the model acquired the ability to make accurate predictions on new data by recognising patterns from previous data, enabling it to generalise effectively. Rigorous evaluation metrics, including Mean mean-squared error and R-squared, were integrated to assess the model's effectiveness in capturing battery degradation patterns. This proposed method establishes a robust framework for predicting battery capacity degradation, providing valuable insights to optimise usage and extend the lifespan of electric vehicle batteries. For the paper, we implemented FPGA as a foundational platform for applying machine learning algorithms. FPGA isa high performance computing platform with low latency and power consumption. A PYNQ-enabled board, easily using Python in Jupyter Notebook, emerged as an ideal platform.

This section delves into the FPGA design considerations for the PYNQ FPGA platform, an open-source framework for designing embedded systems using Xilinx Zynq System on Chip (SoC) FPGA devices. Due to its versatility, it finds applications in diverse fields such as Automotive, Aerospace, These algorithms learn patterns and features that forecast the state of health and capacity degradation over cycles of the Li-ion battery.

2.2 NASA DATASET

This project proposes a novel approach to estimating batteries' State of Health (SOH). The method relies on data-driven techniques and leverages battery ageing information from

the Prognostic Centre of Excellence (PCoE), closely associated with the National Aeronautics and Space Administration. It is essential to monitor battery ageing data chronologically and continuously to properly assess the battery's state of health (SOH). This monitoring process offers significant information on the battery's dynamic conditions. A dedicated battery prognostics testbed incorporates a threshold below the 2.7 V specified by the OEM to simulate deep discharge ageing.

Batteries experience a decrease in lifespan due to the repeated charging and discharging process. The capacity of the batteries decreased from 2 Ah to 1.4 Ah, representing a 30% decrease, which led to the conclusion of the trial. The end-oflife (EOL) requirement was met .Cycles can be classified into impedance, charge, or discharge cycles. Various parameters, such as discharge capacity, time span, temperature, voltage, and current, are closely monitored throughout each cell cycle. This study has focused primarily on the NASA Lithium-ion Batteries dataset, specifically cells B0005, B0006, B0007, and B0018.

2.3 ML IN FPGA INTEGRATION

The project's final phase involves FPGA integration, encompassing implementing capacity degradation code on a PYNQ board. The code, originally developed and implemented in Python, is transformed into a hardware description language (HDL) compatible with the FPGA. The integration begins with selecting an appropriate FPGA board, considering speed, capacity, and connectivity options. Then, the Python code is converted into HDL syntax, considering the appropriate HDL for the FPGA board and tools used. This translation process involves converting Python algorithms into HDL constructs or custom logic.

After generating the HDL code, it undergoes synthesis to transform high-level HDL into low-level gate-level representations. FPGA synthesis tools optimise the code for the target FPGA, considering factors like timing, area utilisation, and power consumption. Subsequently, the gate-level netlist undergoes place-and-route (P&R), where tools map the logic onto FPGA resources, optimising placement and routing to meet timing requirements and minimise signal delays.

Ultimately, the configuration file, typically a bit stream, is loaded onto the FPGA, programming its internal resources to implement the capacity degradation algorithm in hardware.

3 HARDWARE AND SOFTWARE TOOLS

3.1 HARDWARE REQUIREMENT

3.1.1 PYNQ-Z2 BOARD

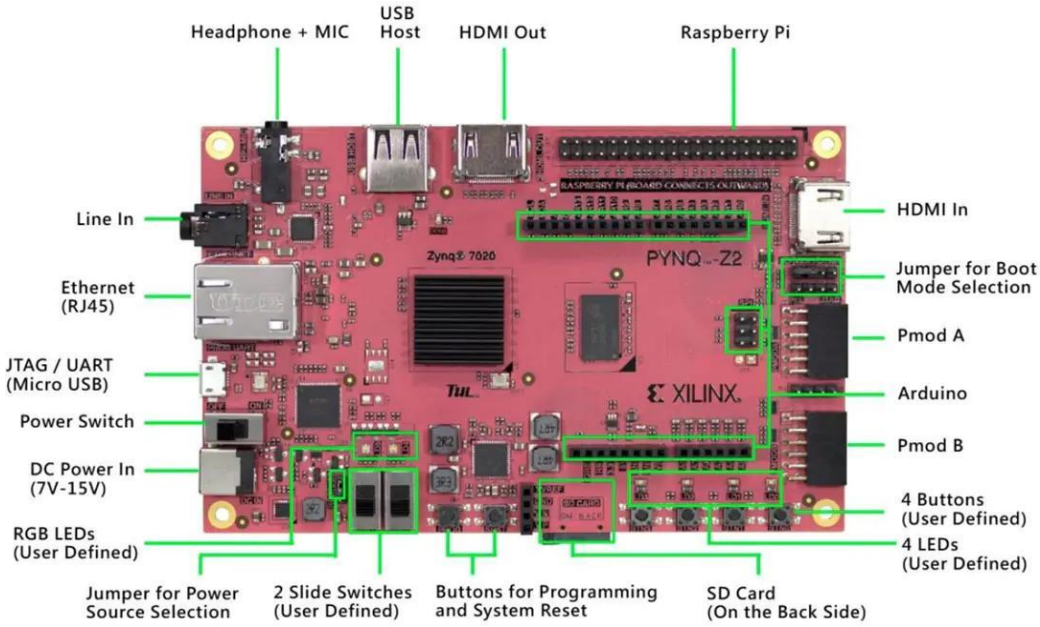

PYNQ Z2 Board

ZYNQ XC7Z020-1CLG400C

- 650MHz ARM® Cortex®-A9 dual-core processor

- Programmable logic 13,300 logic slices, each with four 6-input LUTs and 8 flip-flops 630 KB block RAM 220 DSP slices On-chip Xilinx analog-to-digital converter (XADC)

- Programmable from JTAG, Quad-SPI flash, and MicroSD card

MEMORY AND STORAGE

- 512MB DDR3 with 16-bit bus @ 1050Mbps

- 16MB Quad-SPI Flash with factory programmed 48-bit globally unique EUI- 48/64™ compatible identifier

- MicroSD slot

USB AND ETHERNET

- Gigabit Ethernet PHY
- Micro USB-JTAG Programming circuitry
- Micro USB-UART Bridge
- USB 2.0 OTG PHY (supports host only)

AUDIO AND VIDEO

- 2x HDMI ports (input and output)
- 24bit I2S DAC with 3.5mm TRRS jack
- Line-in with 3.5mm jack

SWITCHES, PUSH-BUTTONS AND LEDS

- 4 push-buttons
- 2 slide switches
- 4 LEDs
- 2 RGB LEDs

EXPANSION CONNECTORS

- 2xPmod ports
- 16 Total FPGA I/O (8 pins on Pmod A are shared with Raspberry Pi connector)
- Arduino Shield compatible connector
- 24 Totals FPGA I/O
- 6 Single-ended 0-3.3V Analog inputs to XADC
- Raspberry Pi connector
- 28 Total FPGA I/O (8 pins are shared with Pmod A).

3.1.2 POWER

The PYNQ-Z2 can be powered from the Micro-USB port (J8), an external power supply, or a battery. The power source is selected by setting jumper J9 (near SW1) to USB or REG (External power Regulator /Battery).

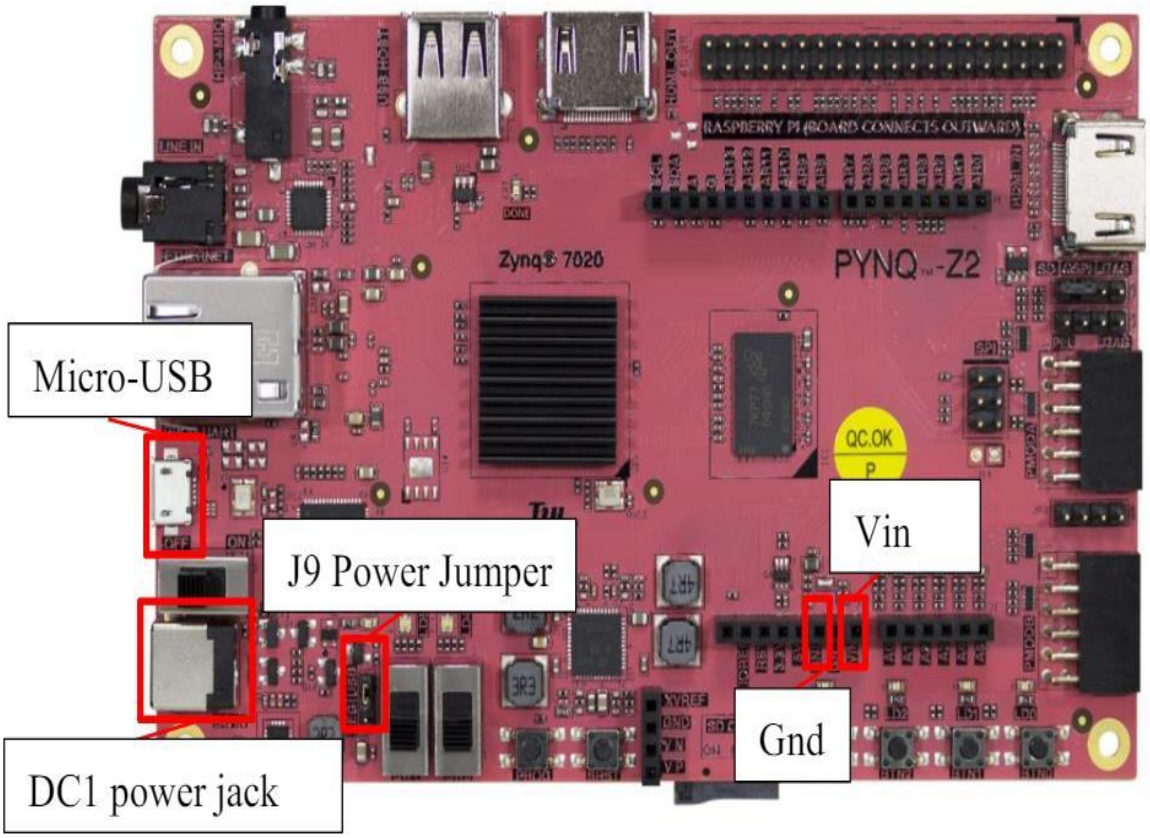

Pin configurations of PYNQ

The Micro USB port connects to a standard USB port and should provide enough power for most designs. More demanding applications may require more power than the USB port can provide.

When more power is required, an external power regulator (coax, center-positive 2.1mm internal-diameter plug) can be connected to the power jack (DC1). The board supports 7VDC to 15VDC (12V recommended). Suitable supplies can be purchased from the TUL website. A battery can also be used to power the PYNQ-Z2 by attaching the positive terminal to the “VIN” pin on the Arduino J7 connector (with jumper J9 set to REG). The negative terminal can be connected to one of the pins labeled GND on J7.

3.1.3 BOOT MODE SELECTION

The PYNQ-Z2 supports MicroSD, Quad SPI Flash, and JTAG boot modes. The boot mode is selected using the Mode jumper (JP1). TO select the boot mode, move the jumper to the appropriate position as indicated by the label on the board

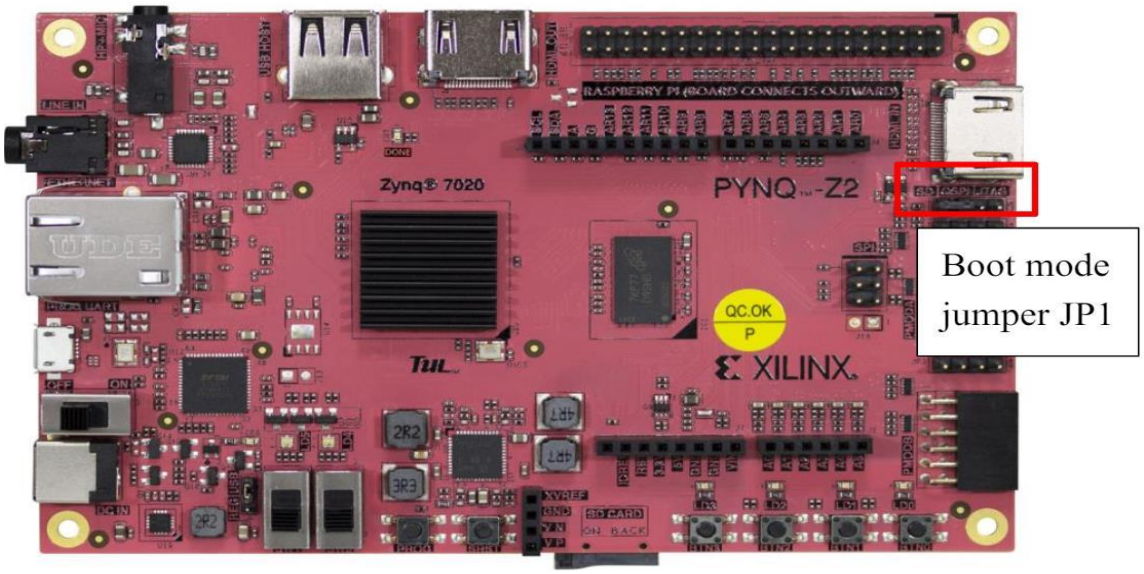

Boot mode Selection

3.1.4 DRAM

The PYNQ-Z2 includes a Micron 256Mx16 DDR3 memory (MT41K512M16HA-125 :A) creating a single rank, 16-bit wide interface with a total capacity of 512MB. The DDR3 is connected to the hard memory controller in the Processor Subsystem (PS). The PS incorporates an AXI memory port interface, a DDR controller, the associated PHY, and a dedicated I/O bank. DDR3 memory interface supports speeds of up to 525 MHz/1050 Mbps on the PYNQ-Z2 board. For best DDR3 performance, DRAM training is enabled for write levelling, read gate, and read data eye options in the PS Configuration Tool in the Xilinx tools. Training is done dynamically by the controller to account for board delays, process variations and thermal drift. The PYNQ-Z2 board files (see section 2) contain the configuration for the DRAM controller which includes optimum starting values for the training process taking into account PCB and trace delays (propagation delays) for the memory signals board delays are specified for each of the byte groups. These parameters are board-specific and were calculated from the PCB trace length reports. The DQS to CLK Delay and Board Delay values are calculated specific to the PYNQ-Z2 memory interface PCB design.

3.1.5 QUAD SPI FLASH

The PYNQ-Z2 features a Spansion S25FL128S Quad SPI neither serial NOR flash.

- 16 MB x1, x2, and x4 support
- Bus speeds up to 104 MHz, supporting Zynq configuration rates @ 100 MHz In Quad SPI mode, this translates to 400Mbs
- Powered from 3.3V

The Multi-I/O SPI Flash memory can be used to initialize and boot the PS subsystem as well as configure the PL subsystem, or as non-volatile code and data storage. The SPI Flash connects to the Zynq-7000 SoC and supports the Quad SPI interface. This requires connection to MIO [1:6,8] as outlined in the Zynq datasheet.

MIO Pin	Name
1	CS
2	DQ0
3	DQ1
4	DQ2
5	DQ3
6	SCLK
7	VCFG0
8	SLCK FB

SPI Flash MIO pin mapping

Quad-SPI feedback mode is used, thus qspi_sclk_fb_out/MIO [8] is left to freely toggle and is connected only to a 20K pull-up resistor to 3.3V. This allows a Quad SPI clock frequency greater than FQSPICLK2.

3.1.6 USB HOST

The PYNQ-Z2 includes a TI TUSB1210 USB 2.0 PHY with an 8-bit ULPI interface connected to the Zynq PS USB 0 controller (MIO [28-39]). The PHY features a HS-USB Physical Front-End supporting speeds of up to 480Mbs. The USB interface is configured to

act as an embedded host. USB OTG and USB device modes are not supported. One of the Zynq PS USB controllers can be connected to the appropriate MIO pins to control the USB port.

MIO Pin	Name	MIO Pin	Name
11	USB	34	DATA2
28	DATA4	35	DATA3
29	DIR	36	CLK
30	STP	37	DATA5
31	NXT	38	DATA6
32	DATA0	39	DATA7
33	DATA1	46	RESETN

USB MIO pin mapping

3.1.7 ADAU1761 AUDIO CODEC

The PYNQ-Z2 has an Analog Devices ADAU1761 audio codec. It allows for stereo 48 KHz record and playback. Sample rates from 8KHz to 96KHz are supported. Additionally, the ADAU1761 provides digital volume control. The Codec can be configured using Analog Devices Sigma Studio™ for optimizing audio for specific acoustics, numerous filters, algorithms and enhancements.

3.1.8 MICROSD

The PYNQ-Z2 has a MicroSD slot (SD1). An SD card can be used to boot the board, or for applications that require non-volatile external memory storage. The PS IOP controller SDIO 0 is wired to this port via MIO [40-47]. The pinout can be seen in Table 7.1. The peripheral controller supports SDIO host mode with 1-bit and 4- bit SD transfer modes. SPI mode is not supported. The Zynq PS UART control can be connected to the appropriate MIO

pins to control the MicroSD port The maximum clock frequency is 50 MHz which supports both low-speed and highspeed cards. A Class 4 MicroSD card or better is recommended.

MIO Pin	Name
41	CCLK
42	CMD
43	D0
44	D1
45	D2
46	D3
47	CD

SD MIO pin mapping

3.1.9 ETHERNET PHY

The PYNQ-Z2 has a Realtek RTL8211E-VL PHY supporting 10/100/1000 Ethernet. The PHY is connected to the Zynq RGMII controller. The auxiliary interrupt (INTB) and reset (PHYRSTB) signals connect to MIO pins MIO10 and MIO9, respectively. One of the Zynq PS Ethernet controllers can be connected to the appropriate MIO pins to control the Ethernet port.

MIO Pin	Name	MIO Pin	Name
9	Ethernet Reset	23	RXD0
10	Ethernet Interrupt	24	RXD1
16	TXCK	25	RXD2
17	TXD0	26	RXD3
18	TXD1	27	RXCTL
19	TXD2	52	MDC
20	TXD3	53	MDIO
21	TXCTL		
22	RXCK		

Ethernet MIO pin mapping

The Zynq does not need to be configured for the PHY to establish a connection. After power-up the PHY starts with Auto Negotiation enabled, advertising 10/100/1000 link speeds

and full duplex. The PHY will automatically establish a link if there is an Ethernet-capable partner connected. There are two status LEDs on the RJ-45 connector that indicate traffic activity and link status. Table 9.1 shows the default behaviour.

LED	Color	Description
Link LED (Right)	Green	● Blinking: Transmitting or Receiving
Act LED (Left)	Yellow	● Blinking: There is activity on this port. ● Off: No link is established.

Ethernet status LEDs

3.1.10 MAC Address

A one-time-programmable (OTP) region of the Quad-SPI flash has been factory programmed with a 48-bit globally unique EUI-48/64™ compatible identifier. The OTP address range [0x20;0x25] contains the identifier with the first byte in transmission byte order being at the lowest address. Refer to the Flash memory datasheet for information on how to access the OTP regions. When using the PYNQ framework, Ethernet is automatically handled in the boot-loader, and the Linux system is automatically configured to use this unique MAC address.

3.1.11 MICRO USB PORT

The PYNQ-Z2 includes an FTDI FT2232HL USB-UART bridge (attached to connector J8 PROG UART) that supports USB-JTAG, USB-UART. The PYNQ-Z2 can also be powered from the Micro USB port. The USB_UART allows PC applications to communicate with the board using standard COM port commands (or the tty interface in Linux and MacOS). The Zynq PS UART 0 controller is used to connect to the UART device. One of the Zynq PS UART controllers can be connected to the appropriate MIO pins to control the UART port**.**

MIO Pin	Name
14	UART Input
15	UART Output

UART MIO pin mapping

3.1.12 Driver

The driver for the USB_UART should be automatically installed when the board is connected to a computer using Windows 7 or later operating system, and recent versions of Linux and MacOS.

3.1.13 HDMI PORTS

The PYNQ-Z2 contains two unbuffered HDMI ports connected directly to the PL. The board labels indicate one HDMI port as input and the other port as output, but as both ports are connected to PL pins, the designer can choose to use each of these ports as input or output. Both ports use HDMI type-A receptacles with the data and clock signals terminated and connected directly to the Zynq PL. The 19-pin HDMI connectors include three differential data channels, one differential clock channel five GND connections, a one-wire Consumer Electronics Control (CEC) bus, a two-wire Display Data Channel (DDC) bus, a Hot Plug Detect (HPD) signal, a 5V signal capable of delivering up to 50mA, and one reserved (RES) pin. All non-power signals are connected to the Zynq PL with the exception of RES. The PYQN FPGA (Field-Programmable Gate Array) is a hardware platform that allows you to implement custom digital circuits. HDMI (High-Definition Multimedia Interface) ports are commonly used for connecting devices like computers, gaming consoles, and Blu-ray players to monitors, TVs, or projectors.

Pin/Signal	J11 (source) J18		J10 (sink)	
	Description	FPGA pin	Description	FPGA pin
D[2]_P, D[2]_N	Data output	J18, H18	Data input	N20, P20
D[1]_P, D[1]_N	Data output	K19, J19	Data input	T20, U20
D[0]_P, D[0]_N	Data output	K17, K18	Data input	V20, W20
CLK_P, CLK_N	Clock output	L16, L17	Clock input	N18, P19
CEC	Consumer Electronics Control bidirectional	G15	Consumer Electronics Control bidirectional	H17
SCL, SDA	DDC bidirectional	B9,B13	DDC bidirectional	U14, U15
HPD/HPA	Hot-plug detect input (inverted)	R19	Hot-plug assert output	T19

HDMI pin descriptions and PL pin locations

HDMI protocol. This IP core translates the digital signals used by the FPGA into the signals required by the HDMI standard.

3.1.14 LEDS, BUTTONS, SWITCHES

The PYNQ-Z2 board includes 2 tri-colour LEDs, 2 dipswitches, 4 push buttons, and 4 individual LEDs connected to the PL.

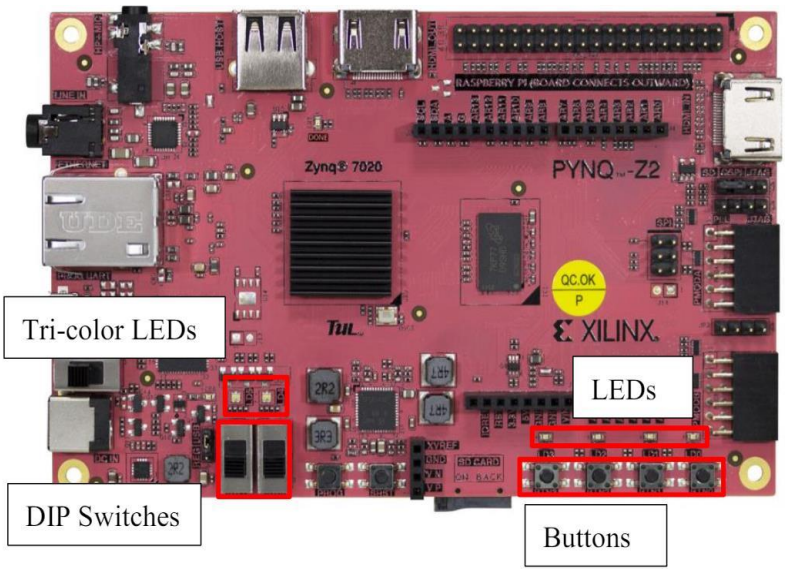

PYNQ Z2 for DIP Switches

Push-buttons

The four push buttons generate logic high on the corresponding PL pin when pressed.

Signal Name	PL PIN
BTN0	D19
BTN1	D20
BTN2	L20
BTN3	L19

Push Button PL pin mapping

Tri colour LEDs

Each of the 2 tri-colour LEDs consists of three internal Reg, Blue Green LEDs. The input signals to the internal RGB LEDs are driven by the Zynq PL through a transistor, which inverts the signals.

Signal Name	PL PIN
LD4 Blue	L15
LD4 Red	N15
LD4 Green	G17
LD5 Blue	G14
LD5 Red	M15
LD5 Green	L14

Push Button PL pin mapping

The tri-colour LEDs are high intensity. It is recommended to use pulse-width modulation (PWM) when driving the tri-colour LEDs nd to aid driving the tri-colour LEDs with more than a 50% duty cycle. Using PWM also allows the LED to support a wide range of colours by adjusting the duty cycle of each colour.

3.1.15 BOARD RESET SIGNALS

SRST is the external system reset. It resets the Zynq device without disturbing the debug environment. System reset erases all memory content within the PS, including the OCM. The PL is also cleared during a system reset. System reset does not cause the boot mode strapping pins to be re-sampled. The SRST button also causes the CK_RST signal to toggle in order to trigger a reset on any attached shields. The Zynq PS supports external power-on reset, a master reset of the whole chip. The TPS65400 power regulator drives a PGOOD signal to hold the system in reset until all power supplies are valid. The PROG push switch, labeled PROG, enables Zynq PROG_B. This resets the PL and causes DONE to be de-asserted. The PL will remain unconfigured until it is reprogrammed by the processor or via JTAG.

3.1.16 PMOD PORTS

The VCC and Ground pins can deliver up to 1A of current

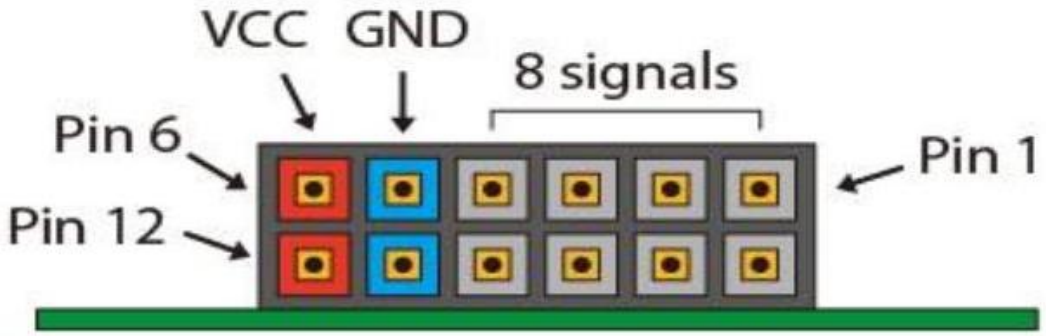

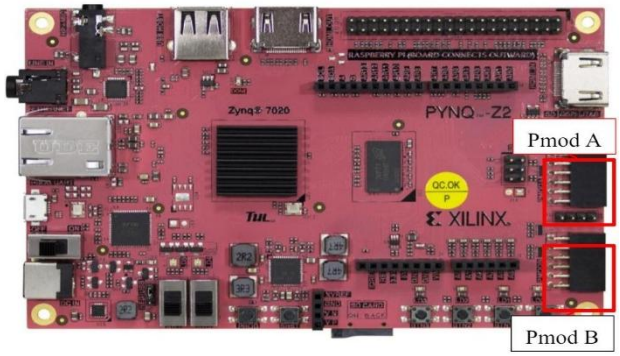

Pmod ports are 2×6, right-angle, 100-mil spaced female connectors that mate with standard 2×6 pin headers. Each 12-pin Pmod port provides two 3.3V VCC signals (pins 6 and 12), two Ground signals (pins 5 and 11), and eight logic signals.

3.1.17 ARDUINO SHIELD CONNECTOR

The Arduino shield connector has 26 pins connected to the Zynq PL. The pins can be used as GPIO. Compatible Arduino shields can be connected to the PYNQZ2 board via this header to extended functionality. Note that as the Arduino header is connected to the PL, a design with appropriate controllers must be loaded before the Arduino header can be used. Six of the Arduino pins (labeled A0-A5) can also be used as single-ended analog inputs with an input range of 0V-3.3V, and another six (labeled AR0-AR13) can be used as differential analog inputs.

3.1.18 DIGITAL I/O

The pins connected directly to the Zynq PL can be used as general-purpose inputs/outputs. These pins include the pins labelled I2C (SCL, SDA), SPI (SS, SCL, MISO, MOSI), and general purpose I/O pins. There are 200 Ohm series resistors between the FPGA and the digital I/O pins to help provide protection against accidental short circuits.

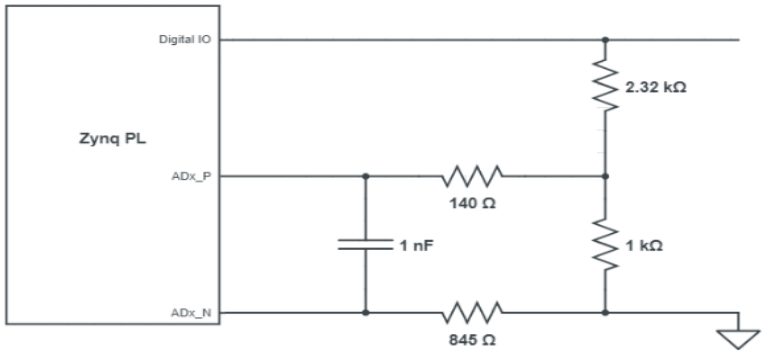

Single-Ended Analog Inputs

This circuit allows the XADC module to accurately measure any voltage between 0V and 3.3V (relative to the PYNQ-Z2's GND) that is applied to any of these pins. If you wish to use the pins labeled A0-A5 as Digital inputs or outputs, they are also connected directly to the Zynq PL before the resistor divider circuit. The pins labeled V_P and V_N are connected to the VP_0 and VN_0 dedicated analog inputs of the FPGA. This pair of pins can also be used as a differential analog input with voltage between 0-1V, but they cannot be used as Digital I/O.

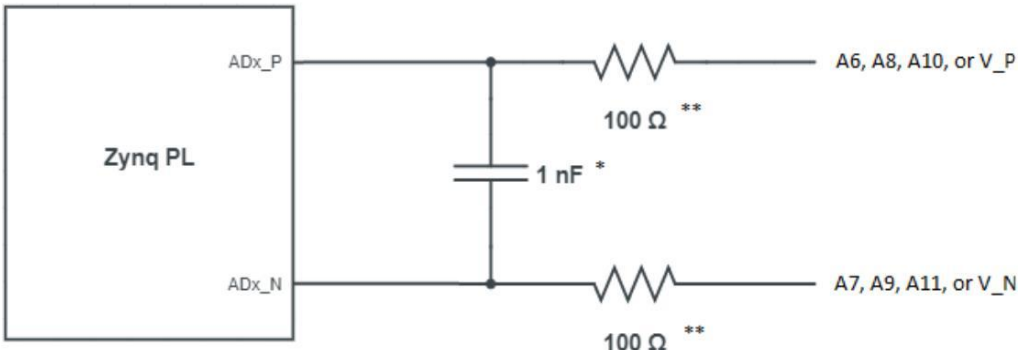

Differential Analog Inputs

For more information on the XADC, see the Xilinx document titled “7 Series FPGAs 26 and Zynq-7000 SoC XADC Dual 12-Bit 1 MSPS Analog-to-Digital Converter”.

PMODA Share Pins				JA3_P	JA1_N	JA2_P										JA1_P	JA4_N	JA4_P	
G	W9	Y8	W8	U18	Y19	Y16	G	W10	V10	V8	V	U8	V7	U7	G	Y18	W19	W18	V
39	37	35	33	31	29	27	25	23	21	19	17	15	13	11	9	7	5	3	1
40	38	36	34	32	30	28	26	24	22	20	18	16	14	12	10	8	6	4	2
Y9	A20	B19	G	B20	G	Y17	U19	F19	F20	G	Y7	W6	G	C20	Y6	V6	G	V	V
PMODA Share Pins						JA2_N	JA3_N												

PULL HIGH: pin 3, 5, 27, 28,

G	Ground
V	3.3V
V	5V
...	Raspberry Pi header pin number
...	Zynq Pin

Table 22 Raspberry Pi header pin layout and Zynq PL pin assignments

NOTE : SHARE PIN (REFERENCE TABLE)

XC7Z020 PIN NAME	PMODA PIN NAME	RASPBERRY PI PIN NAME
IO_L17P_T2_34	JA1P	RPIO_04_R
IO_L17N_T2_34	JA1N	RPIO_05_R
IO_L7P_T1_34	JA2P	RPIO_SD_R
IO_L7N_T1_34	JA2N	RPIO_SC_R
IO_L12P_T1_MRCC_34	JA3P	RPIO_06_R
IO_L12N_T1_MRCC_34	JA3N	RPIO_07_R
IO_L22P_T3_34	JA4P	RPIO_02_R
IO_L22N_T3_34	JA4N	RPIO_03_R

Raspberry Pi header pin layout and Zynq PL pin assignments

3.2 SOFTWARE TOOLS

Jupyter Notebook is an open-source web application that allows users to create and share documents containing live code, equations, visualizations, and narrative text. It has become a standard tool within the data science community for various reasons, particularly in the application of machine learning models, such as those predicting the performance and degradation of lithium-ion batteries. When applied in a Python environment on an FPGA, such as PYNQ (Python Productivity for Zynq), Jupyter Notebook serves as an invaluable tool for several reasons.

Interactive Development Environment Jupyter Notebooks provide an interactive environment where machine learning practitioners can write code and observe the output in real time, making it easier to test hypotheses, visualize data, and debug code quickly. In the context of lithium-ion battery life prediction. Iterative Exploration the iterative nature of Jupyter Notebooks is ideal for the exploratory phase of machine learning, where data scientists can preprocess, analyse, and visualize battery usage and degradation data step-by-step.

Immediate Feedback Visualizations like degradation curves, capacity plots, and charge/discharge cycle graphs can be generated and modified on the fly, providing immediate feedback that can guide further analysis. Documentation and Reproducibility One of the key strengths of Jupyter Notebook is its ability to combine code, output, and descriptive text in a single document. Narrative Context Explanatory text using Markdown and LaTeX can be interleaved with code, allowing researchers to document their methodology and findings clearly. This is crucial when developing predictive models where the logic and assumptions need to be transparent.

Reproducibility Notebooks can be shared with other researchers who can then execute the code in the same sequence, ensuring reproducibility. This is important in scientific research, where results must be verifiable. Collaboration Jupyter Notebooks are designed to be easily shareable through email, GitHub, or other platforms, which enhances collaboration

Sharing Results Colleagues can view the rendered notebook without the need to run code, making it easier to share results and insights with non-technical stakeholders.

Collaborative Editing Tools like JupyterHub and Google Colab allow multiple users to work on the same notebook simultaneously, further improving collaborative efforts. Integration with PYNQ-FPGA PYNQ (Python Productivity for Zynq) is an open-source framework that enables the development and programming of Zynq FPGAs exclusively using Python. This integration offers several advantages. High-Level Programming Python is a high-level programming language, which makes it accessible to researchers and developers without a background in hardware description languages (HDLs).

FPGA Acceleration Machine learning models can benefit from the parallel processing capabilities of FPGAs, which can accelerate computations such as matrix multiplications that are common in battery life prediction models. PYNQ Libraries PYNQ provides libraries and IP (Intellectual Property) cores that are optimized for FPGAs. Data scientists can leverage these to implement high-performance predictive models without delving into low-level FPGA design. Visualization and Model Tuning Jupyter Notebooks support numerous visualization libraries like Matplotlib, Seaborn, and Plotly, which are essential for analyzing battery data: Data Insights: Visualizing the state of health (SOH) and other battery characteristics can reveal patterns that are not obvious from raw data.

Model Tuning the ability to plot learning curves and validation errors in real time helps in fine-tuning the hyperparameters of machine learning models for better accuracy and performance. Streamlined Workflow The use of Jupyter Notebooks streamlines the workflow from data pre-processing to model deployment: End-to-End Process a single notebook can contain the entire workflow of a model, from data loading and cleaning to training and evaluation. Quick Prototyping: The ease of trying out different models and techniques makes Jupyter Notebook an ideal platform for prototyping and experimentation. In summary, Jupyter Notebook is an indispensable tool in the field of machine learning for the predictive analysis of lithium-ion batteries. When used in conjunction with PYNQFPGA, it provides a powerful environment that combines the ease of Python with the performance benefits of hardware acceleration; all while fostering a collaborative, reproducible, and well-documented approach to research and development.

3.2.1 MODULES USED

NUMPY

Numpy used in this project for Numerical Computing Foundation Array Operations,NumPy provides support for large, multi-dimensional arrays and matrices, which

are essential for handling numerical data efficiently. Mathematical Functions: It includes mathematical functions that operate on these arrays, enabling complex calculations required for data preprocessing and model development. Performance: As NumPy operations are vectorized, they are highly optimized and performant, which is critical for large-scale battery degradation analyses.

PANDAS

Data Manipulation and Analysis Data Structures: Pandas introduces two key data structures—DataFrame and Series—that are used for storing and manipulating tabular data. Data Preprocessing: It provides tools for cleaning, transforming, and aggregating data, which are necessary steps before applying machine learning algorithms. Data Exploration: Pandas also offers data filtering, grouping, and summary statistics functionalities, making it easier to explore and understand battery data.

SCIKIT-LEARN

Machine Learning Algorithms and Utilities Model Training: Scikit-learn includes a wide range of supervised and unsupervised learning algorithms, which can be employed to train predictive models on historical battery data.

Cross-validation: It offers tools for splitting data into training and test sets and conducting k-fold cross-validation to assess model performance.

Model Evaluation: Scikit-learn provides various metrics and scoring methods, such as MAE and RMSE, to evaluate the accuracy of the models in predicting battery degradation.

KERAS

Neural Network API for High-Level Model Construction Model Design: Keras is a high-level neural networks API that facilitates the rapid design and prototyping of deep learning models.

Abstraction: It abstracts away much of the complexity of constructing neural networks, making it accessible to use without sacrificing functionality.

Flexibility: Keras allows for easy customization of neural network layers, activation functions, and optimizers, which can be tailored to the specific needs of battery degradation modelling.

PYTORCH

Deep Learning Framework with Dynamic Computation Graphs Dynamic Graphs: Unlike Keras, PyTorch uses dynamic computation graphs, which allow for more flexibility in model architecture and are particularly useful for complex models that require conditional operations.

Performance: PyTorch integrates seamlessly with PYNQ-FPGA, allowing for the optimization and acceleration of deep learning operations on hardware.

Research-Friendly: It is favored in the research community due to its ease of use and debugging capabilities, making it ideal for experimenting with new approaches in battery degradation modelling.

MATPLOTLIB

Visualization Library for Creating 2D Plots and Graphs Data Visualization: Matplotlib is a plotting library that can be used to create a wide range of static, animated, and interactive visualizations. Insightful Plots: For battery degradation studies, Matplotlib can be utilized to plot capacity degradation curves, charge/discharge cycles, and other key metrics that provide insights into battery health.

Reporting: The visualizations generated by Matplotlib can be included in reports and presentations to communicate findings and model results effectively. In the context of a PYNQ-FPGA project, these libraries work together to enable data scientists and engineers to efficiently process data, construct and evaluate machine learning models, and visualize the results. The integration with PYNQ-FPGA allows for leveraging the accelerated computing capabilities of FPGA hardware, which can be critical for computationally intensive tasks like training complex neural network models on large datasets of battery cycle data.

4 METHODOLOGIES

This module illustrates the paper's workflow. It encompasses several vital processes. Initially, the NASA PCoE dataset, provided as a Matrix file, undergoes conversion for machine learning purposes. Subsequently, meticulous pre-processing involves cleaning, transformation, and feature preparation. This refined dataset is the foundation for subsequent analysis and modelling, including removing unwanted features and extracting important ones.

This paper uses the Random Forest Regressor model to predict the degradation of lithium-ion battery capacity.

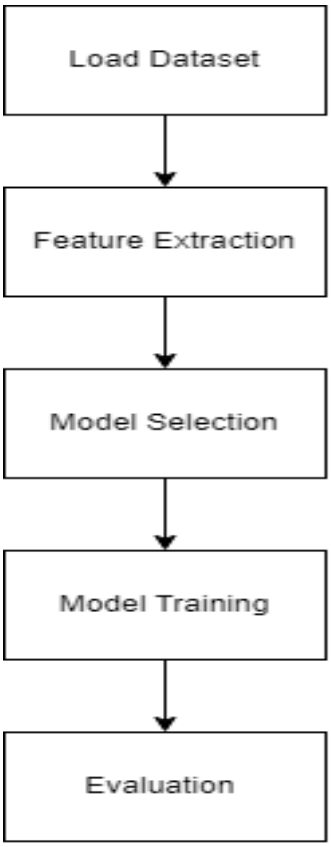

Proposed Method Module

It is expertise in effectively managing intricate data connections, specifically in capturing the intricate patterns found in the electrochemical behaviour of batteries. Leveraging ensemble learning, the model mitigates overfitting and provides robust predictions. It is well-suited for optimising electric vehicle battery usage and extending its lifespan.

A ten-fold cross-validation process is employed to ensure a comprehensive evaluation of the model's performance and its ability to apply to different scenarios. This technique involves dividing the dataset into ten equal parts, training the model on nine portions, and assessing its performance on the remaining one. Repeating the procedure ten times requires a comprehensive evaluation of the model's efficacy. The Adam algorithm, an adaptive optimisation algorithm, effectively optimises the model's parameters. The project's final phase involves FPGA integration, encompassing implementing capacity degradation code on a PYNQ board. The code, originally developed and implemented in Python, is transformed into a hardware description language (HDL) compatible with the FPGA. The integration

begins with selecting an appropriate FPGA board, considering speed, capacity, and connectivity options. Then, the Python code is converted into HDL syntax, considering the appropriate HDL for the FPGA board and tools used. This translation process involves converting Python algorithms into HDL constructs or custom logic. After generating the HDL code, it undergoes synthesis to transform high-level HDL into low-level gate-level representations. FPGA synthesis tools optimise the code for the target FPGA, considering factors like timing, area utilisation, and power consumption. Subsequently, the gate level net list undergoes place-and-route (P&R). Ultimately, the configuration file, typically a bit stream, is loaded onto the FPGA, programming its internal resources to implement the capacity degradation algorithm in hardware.

5 RESULTS AND DISCUSSION

5.1 EXPERIMENTAL SETUP

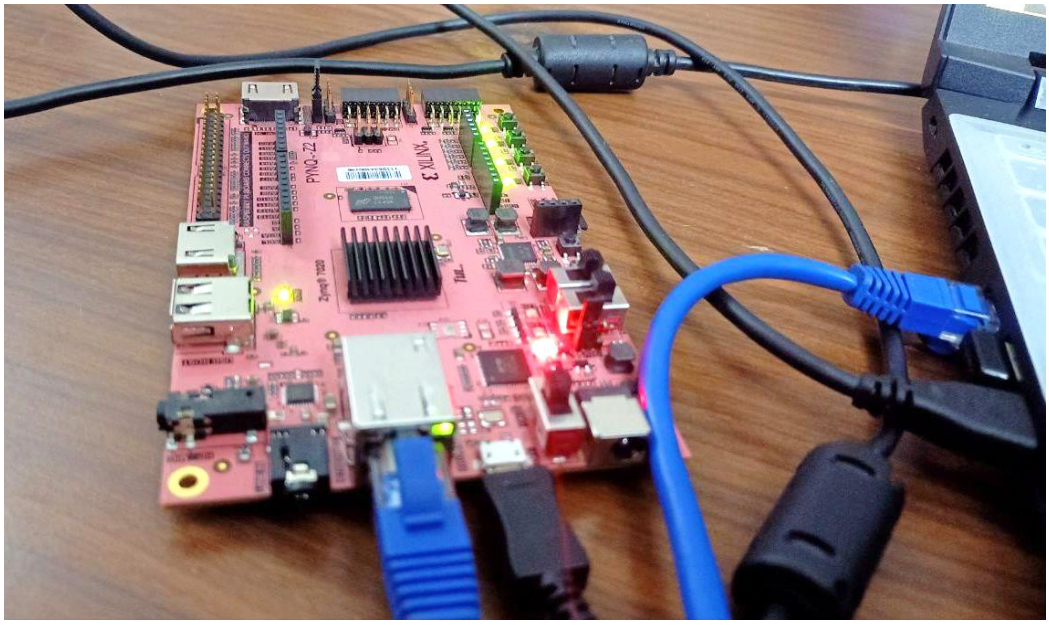

PNYQ board setup

The integration of the Xilinx PYNQ board is instrumental in augmenting the capabilities and performance of the FPGA-based project aimed at analyzing and predicting Lithium-Ion Battery Degradation, utilizing datasets provided by NASA. By harnessing the power of its FPGA architecture combined with the ease of Python programmability, the PYNQ board enables researchers and developers to effectively design and execute real-time data processing and predictive analytics tailored specifically to the nuances of battery health monitoring.

The board's hardware acceleration feature plays a critical role in expediting computationally demanding tasks such as data preprocessing, statistical analysis, and machine learning model execution. This significant boost in processing speed is key to achieving real-time analytics, which is crucial for monitoring the health and predicting the lifespan of Lithium-Ion batteries. Moreover, the board's seamless integration with the Python ecosystem allows for rapid prototyping, debugging, and testing of predictive models using well-known libraries and tools. This leads to an efficient development process and a shorter time to-deployment for predictive maintenance applications.

By interfacing with battery management systems and sensors, the PYNQ board processes real-time battery operation data, applying FPGA-based acceleration to data cleansing, normalization, and feature extraction tasks. This preprocessing enhances the overall quality and reliability of the data, which feeds into advanced predictive models. Critical stages of the predictive pipeline, such as regression analysis, anomaly detection, and state of health (SOH) estimation, are optimized through hardware implementations on the FPGA. These optimizations ensure minimal latency in data processing and allow high-throughput performance even when dealing with the extensive battery datasets provided by NASA.

In conclusion, the Xilinx PYNQ board emerges as a highly versatile and capable platform for the FPGA-based Battery Degradation Project. It empowers the project to realize robust, real-time monitoring and predictive capabilities for Lithium-Ion batteries, significantly enhancing the accuracy, efficiency, and reliability of battery lifespan predictions and health assessments. This not only contributes to the longevity and safety of battery-powered devices but also supports the advancement of sustainable energy solutions.

5.2 RESULTS

This paper examines the capacity of a lithium-ion battery by subjecting it to multiple charge and discharge cycles. Displays the resulting plot, showcasing the battery's current capacity as a curve representing discharge cycles versus capacity. The model uses past data to predict the RUL or remaining useful life. Consequently, we initially assess the model's performance using evaluation metrics such as Relative Error (RE), Mean Absolute Error (MAE), and Root Mean Square Error (RMSE). It is a beneficial metric used in Regressor model training's performance. Table 1 displays the performance of the acquired trained model.

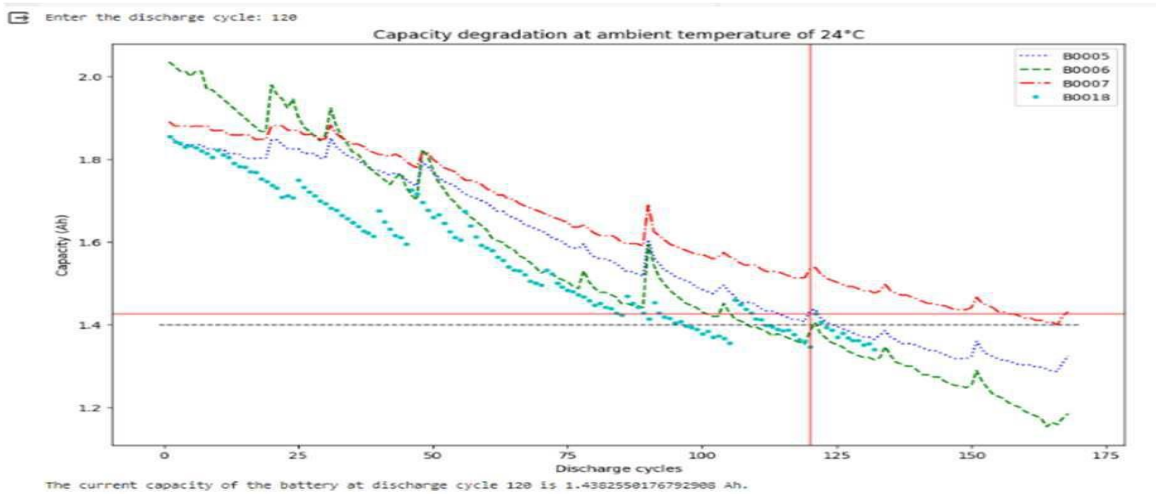

Capacity degradation Curve

Evaluation metrics

METRICS	VALUES
MAE	0.07010
MSE	0.01487
RMSE	0.12197

5.2.1 EVALUATION METRICS

A. Mean Squared Error (MSE)

The mean squared error (MSE) is a statistical metric that quantifies the discrepancy between observed and predicted values. An evaluation is conducted on the model's performance, emphasising imposing stricter penalties for more significant errors.

B. Mean Absolute Error (MAE)

When comparing expected and actual data, MAE finds the mean absolute difference. It calculates the mean error size independent of the direction of the faults.

C. Root Mean Squared Error (RMSE)

In regression analysis, root-mean-squared error (RMSE) measures a model's predictive power. As a whole, it quantifies how much of a gap there is between expected and actual values.

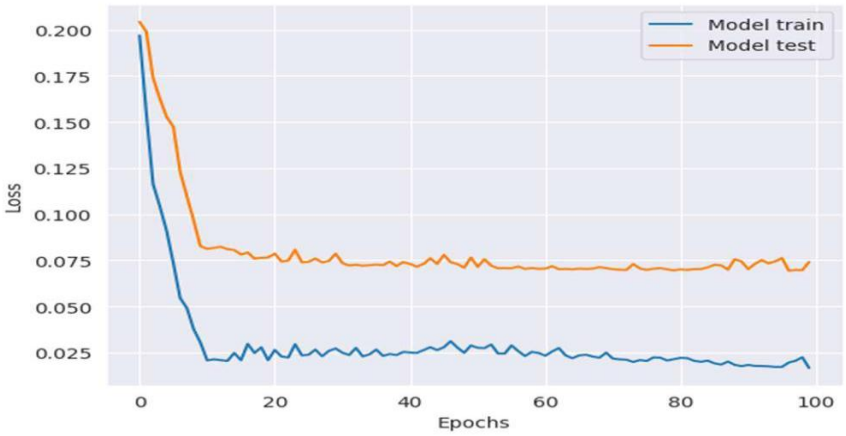

Model loss

The model iteratively adjusts its weights in each epoch based on the error between predicted and actual values, progressively enhancing its performance. The optimisation process may necessitate multiple epochs to fine-tune the model, and the number of epochs is a hyperparameter influencing training effectiveness. The Adam optimisation algorithm ensures continuous learning, dynamically adapting to evolving data patterns. Privacy-preserving techniques and ensemble learning further enhance the model's reliability and security. Fig. 6 displays the model loss of a trained model. Its capacity to conduct its cross-validation process on time and engage in an iterative feedback loop underscores its robustness and efficacy when applied in real-world scenarios. These collective features contribute to the model's seamless integration into electric vehicle workflows, ensuring its effectiveness.

KNEE OSTEOARTHRITIS DETECTION AND CLASSIFICATION USING X-RAYS

YAZHINI S RUBIGA S A

ABSTRACT

Detection of knee osteoarthritis (OA) through X-ray imaging is vital for diagnosing and managing this prevalent joint disorder. X-rays reveal characteristic features such as joint space narrowing, osteophyte formation, and bone changes, aiding in disease assessment and severity grading using systems like the Kellgren-Lawrence scale. While X-rays offer accessibility and affordability, they have limitations in capturing soft tissue abnormalities and dynamic changes. Advancements in technology, including digital radiography and computer-aided detection, enhance accuracy. Therefore, current management strategies focus on symptom alleviation unless the severity of the condition necessitates surgical intervention, such as joint replacement. Despite limitations, X-ray imaging remains a cornerstone in knee OA diagnosis, guiding treatment decisions and improving patient care. Detecting knee osteoarthritis (OA) through X-ray imaging has become a cornerstone in the diagnosis and management of this prevalent musculoskeletal disorder. Osteoarthritis, characterized by the progressive degeneration of joint cartilage and underlying bone changes, primarily affects weight-bearing joints such as the knees. While X-rays cannot directly visualize cartilage, they offer valuable insights into the extent of joint degeneration and help clinicians assess disease severity and progression. Leveraging transfer learning techniques to adapt pre-trained YOLO to the task of knee OA detection. Transfer learning allows models to leverage knowledge gained from training on datasets for related tasks, thereby accelerating model convergence and improving performance with limited labeled data. Our project can able to detect the Knee Osteoarthritis with a good and high accuracy and precision which will explained in detail in this report. One of the primary objectives of X-ray imaging in knee osteoarthritis detection is to identify radiographic signs indicative of the disease.

1 INTRODUCTION

Osteoarthritis (OA) stands as the prevailing type of arthritis globally and ranks among the primary causes of disability. This degenerative joint ailment affects an estimated 260 million individuals worldwide, with over 37 million cases in the United States alone. The elderly, particularly those aged over 67 (constituting around 40% of OA patients), females, individuals grappling with obesity, and African Americans, face the highest risk of

developing OA. As life expectancy rises and obesity rates escalate, the prevalence of OA is poised to surge significantly in the coming years. Such a projection is alarming, considering OA's debilitating impact, which extends to social and economic spheres. This review will discuss the current evidence regarding the pathophysiology of knee osteoarthritis, the current recommendations of treatment, with a special focus on intervention modalities including intra-articular steroids and the new extended-release (ER) presentations of these components.

1.1 Knee Osteoarthritis

The knee, being the largest synovial joint in humans, comprises various components such as osseous structures (distal femur, proximal tibia, and patella), cartilage (meniscus and hyaline cartilage), ligaments, and a synovial membrane. This membrane plays a crucial role in producing synovial fluid, essential for lubrication and nourishment of the avascular cartilage. Despite its pivotal function, the knee is prone to painful conditions, including osteoarthritis (OA), owing to its frequent use and exposure to stress. OA is typically categorized into primary (idiopathic or nontraumatic) and secondary (often resulting from trauma or mechanical misalignment) forms based on its study. Traditionally viewed as a degenerative cartilage disease, recent evidence underscores its multifactorial nature, involving trauma, mechanical forces, inflammation, biochemical reactions, and metabolic imbalances. Contrary to earlier beliefs, OA doesn't solely affect cartilaginous tissue; instead, it impacts various joint components like the joint capsule, synovium, subchondral bone, ligaments, and peri-articular muscles. These structural alterations manifest as bone remodelling, osteophyte formation, muscle weakening, ligament laxity, and synovial effusion as the disease progresses.

Inflammation in osteoarthritis (OA)

Although the precise role of inflammation in osteoarthritis (OA) remains uncertain, chronic, low-grade inflammation, predominantly mediated by innate immune mechanisms, appears to be significant. Synovitis, characterized by inflammatory cell infiltration into the synovium, is a prevalent feature of OA and tends to worsen with disease severity. Inflammatory mediators present in the synovial fluid, such as plasma proteins, prostaglandins, leukotrienes, cytokines, growth factors, nitric oxide, and complement components, contribute to cartilage degradation by stimulating matrix metalloproteinases and other hydrolytic enzymes. Additionally, white blood cells, notably macrophages and mast cells, react to molecules released from extracellular matrix breakdown, potentially exacerbating tissue damage. Animal studies implicate macrophages in the formation of osteophytes, a characteristic feature of OA.

The body also employs protective molecular mechanisms, including various growth factors (insulin-like growth factor, platelet-derived growth factor, fibroblast growth factor 18, and transforming growth factor β). Unfortunately, these mechanisms are altered in patients with knee OA and may become detrimental to the joint. OA is a progressive and degenerative condition, with little chance of regression or restoration of damaged structures. Therefore, current management strategies focus on symptom alleviation unless the severity of the condition necessitates surgical intervention, such as joint replacement. Several guidelines have been established by various academic and professional societies to standardize and recommend available treatment options. These include publications by the Osteoarthritis Research Society International (OARSI), American College of Rheumatology (ACR), and American Academy of Orthopaedic Surgeons (AAOS).

1.2 Non-pharmacological management

The primary goal of managing osteoarthritis (OA) is to alleviate pain and enhance functionality and overall quality of life. Non-pharmacological interventions are typically the initial approach for treating knee OA. It's essential to address inactivity and encourage physical activity, as lack of movement can accelerate cartilage degeneration. Engaging in light-to-moderate physical activities not only improves joint mechanics and flexibility but also reduces the risk of various health issues such as diabetes, cardiovascular events, falls, and disability. Additionally, physical activity can positively impact mood and self-efficacy. Exercise regimens should be personalized to each patient's capabilities and preferences, avoiding high impact activities and focusing on long-term adherence for optimal outcomes.

Various exercise modalities have demonstrated beneficial effects for knee OA patients and should ideally be performed three times a week, with a minimum of 12 sessions to assess response.

Effects of knee OA

Aerobic/endurance	**Exercise modalities** **Resistance /strength training**	**Balance/ proprioceptive**
Include activities like walking, climbing stairs, and cycling. They can decrease joint tenderness while improving functional status and respiratory capacity. Cycling is especially attractive to patients given the low impact profile. One study	Isometric, isotonic, isokinetic, and dynamic modalities have been studied. Most of them targeting quadriceps, hip abductors, hamstrings, and calf muscles. They improve strength, physical function, and pain levels, with	This includes modalities such as Tai Chi, using slow and gentle movements to adopt different weight baring postures while using breathing techniques.

Pharmacological management

Aerobic/endurance	**Exercise modalities** **Resistance /strength training**	**Balance/ proprioceptive**
Showed a reduction of 10–12% on the physical disability and the knee pain questionnaires.	Similar efficacy and outcomes than aerobic exercises.	

The elderly population, comprising the majority of osteoarthritis (OA) patients, often presents with multiple comorbidities, necessitating careful consideration of potential interactions and adverse effects associated with systemic medications. Historically, cyclooxygenase inhibitors like acetaminophen and NSAIDs have been widely used. However, due to their gastrointestinal, renal, cardiac, and haematological adverse effects, long-term usage is limited. Acetaminophen, in particular, has demonstrated inferior efficacy

compared to NSAIDs and placebo for pain management, prompting some guidelines to refrain from recommending it as a primary treatment for moderate-to-severe OA.

Topical NSAIDs offer a safer alternative, with comparable or slightly lower efficacy than systemic NSAIDs. While short-term studies show superiority over placebo in pain control during the initial week of treatment, their benefits tend to diminish after two weeks. Growing awareness regarding the adverse effects of chronic opioid use has led to a revaluation of their role in OA management. Studies consistently indicate that opioids are not superior to NSAIDs in improving OA pain or WOMAC scores, with the risks often outweighing the benefits. Tramadol, a serotonin and norepinephrine reuptake inhibitor with weak μ opioid receptor agonist properties may be considered for refractory cases due to its lower risk of abuse potential and respiratory depression compared to other opioids.

Duloxetine, approved for diabetic peripheral neuropathy and fibromyalgia, has shown promise in OA treatment, demonstrating superior pain control and functional improvement over placebo when used for more than 10 weeks. Early-stage exercises are widely recognized as valuable therapy for these patients and are recommended by all medical societies. However, other non-surgical treatments have varying efficacy, influenced by factors such as the provider, equipment, and patient characteristics, necessitating careful selection based on the individual clinical scenario.

2 EXISTING SYSTEM

The problem statement revolves around addressing the diagnostic challenges associated with knee osteoarthritis (OA) using X-ray imaging and YOLO-based object detection algorithms. Knee OA is a prevalent condition causing significant morbidity and disability, yet its accurate diagnosis remains challenging due to reliance on subjective clinical assessments and variability in radiographic interpretation. Traditional image analysis methods suffer from limitations such as labour-intensive manual segmentation and subjective feature engineering, highlighting the need for automated and objective approaches.

YOLO-based object detection algorithms offer a promising solution by enabling real-time, end-to-end detection of OA features on X-ray images, including joint space narrowing and osteophyte formation. However, there exists a research gap regarding the application of YOLO-based detection in knee OA diagnosis, warranting further investigation into its feasibility, accuracy, and clinical utility. Thus, the objectives of this study include the development and validation of a YOLO-based knee OA detection system, assessment of its

performance compared to traditional methods, and evaluation of its impact on clinical decision-making and patient outcomes. The significance of this research lies in its potential to advance the field of knee OA diagnosis, improve diagnostic accuracy, reduce variability in interpretation, and ultimately enhance patient care and outcomes. However, ethical considerations related to patient privacy, data security, and informed consent must be addressed, emphasizing the importance of adhering to ethical guidelines and regulatory requirements in conducting research involving medical imaging data. An X-ray of the knee joint in a patient with osteoarthritis reveals narrowing of the inner joint space, indicated by black arrows, attributed to cartilage degeneration and loss. Additionally, curved arrows highlight the presence of degenerative spurs. Conversely, white arrows denote the normal space between the bones.

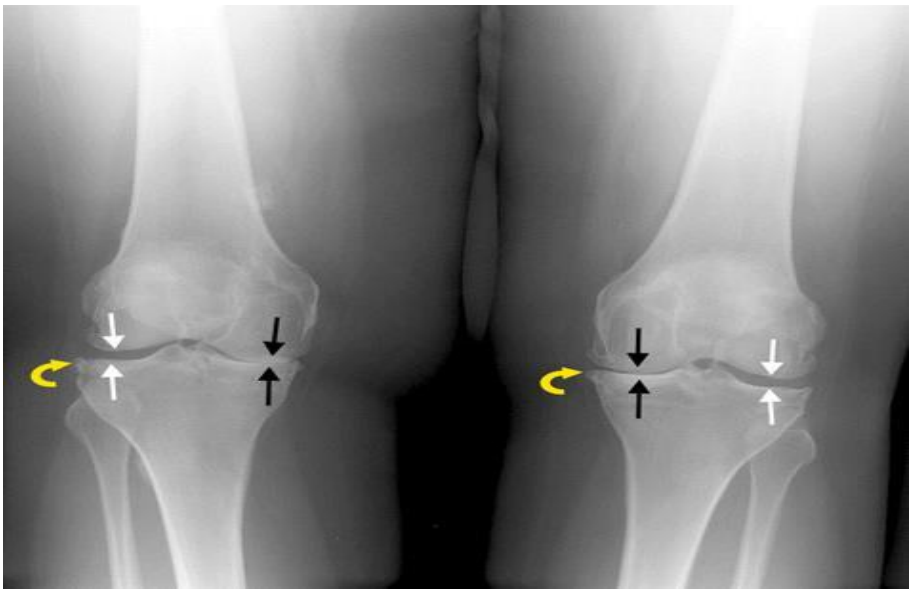

Normal space between the bones

The problem statement encapsulates the pressing need to enhance the diagnostic process for knee osteoarthritis (OA) through the integration of X-ray imaging and YOLO-based object detection algorithms. Knee OA represents a significant healthcare challenge due to its prevalence, impact on patient quality of life, and associated socioeconomic burden. However, current diagnostic approaches often rely on subjective assessments and suffer from interobserver variability, leading to inconsistencies in patient management and treatment outcomes. Addressing these challenges requires the development of objective, automated solutions that can accurately detect OA features on X-ray images in a timely and efficient manner. The complexity of knee OA diagnosis, influenced by various radiographic features,

patient demographics, and clinical symptoms, underscores the need for personalized and standardized diagnostic approaches.

YOLO-based object detection algorithms offer a promising avenue for automating the detection of OA-related abnormalities, including joint space narrowing and osteophyte formation, with real-time efficiency and accuracy. Despite their potential, the application of these algorithms in knee OA diagnosis remains relatively unexplored, necessitating further research to validate their efficacy and clinical utility. The successful implementation of YOLO-based knee OA detection hinges on overcoming several challenges, including technological barriers, regulatory requirements, and clinician acceptance.

Additionally, robust validation studies are essential to assess the performance and generalizability of these algorithms across diverse patient populations and clinical settings. Collaboration among multidisciplinary teams of researchers, clinicians, industry partners, and regulatory agencies is crucial to addressing these challenges and translating research findings into clinical practice effectively. Ultimately, the integration of X-ray imaging and YOLO-based object detection has the potential to revolutionize knee OA diagnosis, improving diagnostic accuracy, reducing variability in interpretation, and enhancing patient outcomes. By providing objective and standardized metrics for OA detection, these automated solutions can streamline clinical workflows, optimize resource utilization, and ultimately transform the management of this prevalent musculoskeletal condition on a global scale.

2.1 Overview of Current Approaches

The recent FDA approval of extended-release triamcinolone acetonide (TA) microspheres (FX006) offers potential advantages over immediate-release CS, including prolonged pain relief and reduced adverse effects. However, uncertainties persist regarding its duration of efficacy beyond 13 weeks. Additionally, the emerging field of regenerative medicine presents promising non-corticosteroid IA therapies, but further research and standardization are imperative for their widespread adoption. Despite being extensively studied and highly prevalent in our population, knee osteoarthritis lacks a clear pathophysiology or a universally effective intervention to manage its symptoms and degeneration. In this chapter, we will explore the current state of knee osteoarthritis (KOA) detection and classification using X-rays. Understanding the existing systems and methodologies is crucial for developing improved approaches to diagnosis and classification.

This chapter will provide an overview of the methods, techniques, and technologies currently employed in the field.

Radiographic Imaging: Traditional X-rays remain the primary modality for imaging knee joints in diagnosing KOA due to their widespread availability, cost effectiveness, and ability to capture structural changes. Manual Assessment: Radiologists and clinicians visually inspect X-ray images to identify characteristic features of KOA, such as joint space narrowing, osteophyte formation, subchondral sclerosis, and bone deformities. X-ray imaging and YOLO-based object detection has the potential to revolutionize knee OA diagnosis, improving diagnostic accuracy, reducing variability in interpretation, and enhancing patient outcomes

2.2 Limitations of Existing Approaches

Scoring Systems: Various scoring systems, such as the Kellgren-Lawrence grading scale and the Osteoarthritis Research Society International (OARSI) atlas, are utilized to classify the severity of KOA based on X-ray findings. Computer-Aided Diagnosis (CAD): CAD systems assist radiologists by automatically analyzing X-ray images and highlighting potential abnormalities associated with KOA. These systems utilize image processing techniques, machine learning algorithms, and deep learning models to improve diagnostic accuracy and efficiency.

Subjectivity: Manual assessment of X-rays is subjective and relies heavily on the expertise of radiologists, leading to inter-observer variability and inconsistency in diagnoses. Sensitivity: Traditional X-ray imaging may lack sensitivity in detecting early-stage KOA changes, particularly in cases with subtle or mild abnormalities. Complexity: Scoring systems and classification criteria can be complex and may not always capture the full spectrum of KOA manifestations, leading to diagnostic challenges. Time-Consuming: Manual assessment and interpretation of X-ray images can be time-consuming, especially in busy clinical settings, delaying diagnosis and treatment initiation.

2.3 Emerging Trends and Technologies

Digital Radiography: Advancements in digital X-ray technology offer improved image quality, enhanced visualization of anatomical structures, and the potential for computerized analysis. In the lateral view of the knee MRI, the image displays the distal portion of the femur, the patella (knee cap), and the proximal region of the tibia. The lateral

meniscus appears as a dark bow-tie shaped structure. Moreover, the patellar tendon is prominently visible at the anterior aspect of the knee, connecting to the patella to the tibia. Additionally, the emerging field of regenerative medicine presents promising non-corticosteroid IA therapies, but further research and standardization are imperative for their widespread adoption.

Artificial Intelligence (AI): AI-based algorithms and deep learning models are being developed to automate KOA detection and classification from X-ray images, promising higher accuracy and efficiency compared to traditional methods. Quantitative Imaging Biomarkers: Researchers are exploring the use of quantitative imaging biomarkers derived from X-rays, such as joint space width measurements and texture analysis, to provide objective assessments of KOA severity. Here are additional points to expand on the emerging trends and technologies in knee osteoarthritis (KOA) detection and classification using X-rays, elaborating on various aspects.

Lateral view of the knee MRI

2.3.1 Digital Radiography Advancements

Patient's knee with Plain x-ray image of fatty marrow in the joint space by advanced radiography advancements. Clinical decision support systems enhance Interdisciplinary collaboration among healthcare providers, facilitating comprehensive patient care and treatment planning for KOA management. High Resolution Imaging: Digital radiography offers higher resolution images compared to traditional film-based X-rays, enabling clearer visualization of subtle joint changes associated with KOA. Cone Beam CT (CBCT): CBCT

technology provides 3D imaging of the knee joint, allowing for comprehensive assessment of bone morphology, cartilage defects, and alignment abnormalities, thereby enhancing diagnostic accuracy. Dual-Energy X-ray Absorptiometry (DEXA): DEXA scans can assess bone mineral density and composition, aiding in the evaluation of osteoporosis-related changes and their impact on KOA progression.

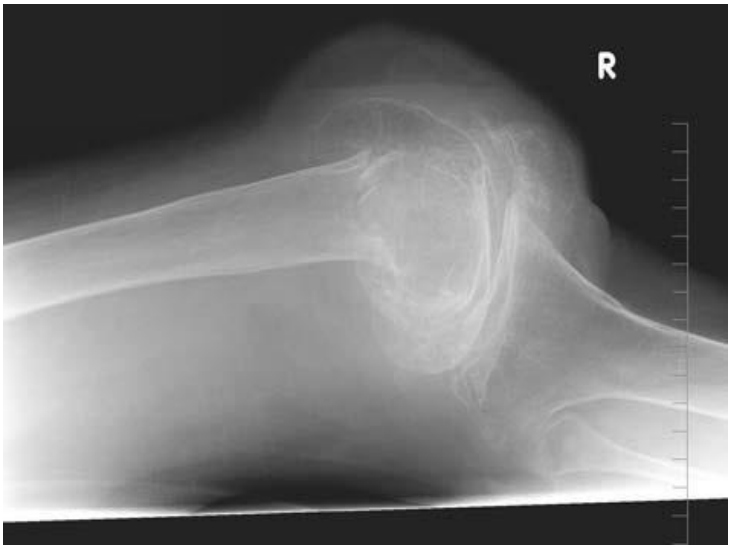

X-ray image of fatty marrow in the joint space

2.3.2 Artificial Intelligence (AI) Applications

Deep Learning Models: Advanced deep learning algorithms, such as convolutional neural networks (CNNs) and recurrent neural networks (RNNs), are being trained on large datasets of X-ray images to automatically detect and classify KOA features with unprecedented accuracy. Transfer Learning: Transfer learning techniques allow AI models to leverage pre-trained networks on related tasks, optimizing performance and reducing the need for extensive training data in KOA detection. Explainable AI: Efforts are underway to develop AI models that provide transparent and interpretable predictions, enabling clinicians to understand the reasoning behind the diagnostic decisions and fostering trust in AI-based diagnostic tools.

Texture Analysis: Texture features extracted from X-ray images, such as entropy, contrast, and homogeneity, serve as quantitative biomarkers for characterizing tissue properties and identifying early signs of KOA progression. Joint Space Width Measurements: Automated measurement techniques enable precise quantification of joint space width on X-rays, facilitating longitudinal monitoring of disease progression and treatment efficacy. Subchondral Bone Analysis: Quantitative assessment of subchondral bone density,

morphology, and microarchitecture provides insights into biomechanical alterations and their association with KOA severity.

Portable X-ray Systems: Compact and portable X-ray machines allow for on-site imaging in clinical settings, reducing patient inconvenience and streamlining the diagnostic workflow for KOA evaluation. Quality control measures, including interannotator agreement checks, communicating with healthcare providers for timely intervention and annotation review processes, can help maintain consistency and accuracy. Handheld Ultrasound Devices: Handheld ultrasound devices offer real time imaging of the knee joint, enabling dynamic assessment of soft tissue structures, synovial fluid, and cartilage thickness as adjunctive tools in KOA diagnosis.

Wearable Sensors: Wearable sensor technologies, such as knee-mounted accelerometers and gyroscopes, provide objective data on joint motion, gait patterns, and physical activity levels, complementing traditional imaging modalities in assessing KOA-related functional limitations. For all this first we have to analyze the normal knee. Here is the Anterior-posterior view of 12-year-old normal knee:

Anterior-posterior view of 12-year-old normal knee

2.3.3 Collaborative Diagnostic Platforms

Integrated Health Information Systems: Integration of X-ray imaging data with electronic health records (EHRs) and clinical decision support systems enhances

interdisciplinary collaboration among healthcare providers, facilitating comprehensive patient care and treatment planning for KOA management. Telemedicine Solutions: Telemedicine platforms enable remote consultation and image interpretation by specialists, extending access to KOA diagnostic expertise to underserved populations and improving healthcare delivery efficiency. Patient Engagement Tools: Interactive patient portals and mobile applications empower individuals with KOA to actively participate in their care by accessing educational resources, monitoring symptom progression, and communicating with healthcare providers for timely intervention and support.

This chapter has provided an overview of the existing systems and methodologies for knee osteoarthritis detection and classification using X-rays. While traditional approaches have served as the cornerstone of KOA diagnosis, they are not without limitations. Emerging trends, such as digital radiography, artificial intelligence, and quantitative imaging biomarkers, hold promise for overcoming these challenges and advancing the field towards more accurate and efficient diagnostic solutions.

3 PROPOSED SYSTEM

3.1 Overview of YOLO Algorithm

YOLOv4 is a state-of-the-art object detection algorithm that builds upon the success of its predecessors, aiming to achieve even higher accuracy and efficiency in real-time object detection tasks. Developed by the research community, YOLOv4 introduces several key improvements and innovations over previous versions, making it a powerful tool for various applications, including autonomous driving, surveillance, and medical imaging. With its modular architecture and configurable hyperparameters, YOLOv4 provides users with the flexibility to tailor the model architecture, training process, and optimization strategies to specific application requirements. Whether it's fine-tuning the model for domain-specific tasks, optimizing for hardware constraints, or integrating with existing systems and frameworks, YOLOv4 offers the versatility needed to address a wide range of object detection challenges.

Additionally, the implementation of data augmentation techniques like Cut Mix and mosaic data augmentation diversifies the training dataset, improving the model's robustness to variations in object appearance and background clutter. As a result, YOLOv4 consistently delivers superior performance in object detection benchmarks, outperforming previous versions and competing algorithms. Despite its impressive accuracy, YOLOv4 maintains high

efficiency and inference speed, making it suitable for real-time object detection applications. Through optimizations in model architecture, hyper parameters, and inference algorithms, YOLOv4 achieves a balance between computational complexity and performance, enabling efficient deployment on resource-constrained devices such as embedded systems, edge devices, and mobile platforms.

3.2 Key features and innovations of YOLOv4 include

Backbone Network Optimization - YOLOv4 incorporates a more powerful backbone network architecture, replacing Darknet-53 with CSPDarknet53, which utilizes Cross-Stage Partial Networks (CSP) to improve feature extraction efficiency and reduce computational complexity. CSPDarknet53 leverages cross-stage feature aggregation to enhance information flow between network layers, facilitating better feature representation and learning capability. Feature Pyramid Network (FPN) Integration - YOLOv4 integrates a Feature Pyramid Network (FPN) into its architecture, enabling multi-scale feature extraction and improving the model's ability to detect objects of varying sizes and aspect ratios.

FPN enhances spatial resolution at different network layers, allowing YOLOv4 to effectively capture context information and localize objects with greater precision. YOLOv4, the latest iteration of the You Only Look Once (YOLO) object detection algorithm, offers several significant advantages over its predecessors, making it a compelling choice for various computer vision tasks. YOLOv4 achieves state-of-theart performance in terms of accuracy and precision, thanks to its advanced architecture design and optimization techniques. By incorporating a more powerful backbone network (CSPDarknet53) and integrating a Feature Pyramid Network (FPN), YOLOv4 enhances feature extraction and context modelling, allowing for better object localization and classification accuracy.

The scalable design of YOLOv4 allows users to adjust the model size and complexity according to specific task requirements and hardware constraints, further enhancing its versatility and applicability in various deployment scenarios. YOLOv4 offers scalability and flexibility in model design and deployment, allowing for customization and adaptation to diverse use cases and environments. With its modular architecture and configurable hyperparameters, YOLOv4 provides users with the flexibility to tailor the model architecture, training process, and optimization strategies to specific application requirements. Whether it's fine-tuning the model for domain-specific tasks, optimizing for hardware constraints, or integrating with existing systems and frameworks, YOLOv4 offers the versatility needed to

address a wide range of object detection challenges. Additionally, the efficient implementation and deployment options of YOLOv4 facilitate seamless integration into production pipelines and real-world applications, enabling rapid development and deployment of computer vision solutions.

3.3 Data Augmentation and Regularization Techniques

YOLOv4 incorporates advanced data augmentation techniques, such as CutMix and mosaic data augmentation, to diversify the training dataset and improve the model's robustness to variations in object appearance and background clutter. Additionally, YOLOv4 implements various regularization techniques, including DropBlock and Mish activation function, to prevent overfitting and enhance model generalization ability. In YOLOv4, dataset preparation plays a crucial role in training the model effectively and achieving optimal performance in object detection tasks. Here's a detailed overview of the dataset preparation process. Data Collection - The first step in dataset preparation is to collect a diverse and representative set of images relevant to the target object detection task.

For knee osteoarthritis (KOA) detection using X-ray images, this involves gathering a large number of knee X-ray images from various sources, including medical databases, research repositories, and healthcare institutions. Care should be taken to ensure that the collected images cover a wide range of scenarios, including different patients, disease severities, imaging techniques, and anatomical variations. Annotation tools such as Labeling, VOTT (Visual Object Tagging Tool), or LabelMe are commonly used to manually annotate the images by drawing bounding boxes around the KOA features and assigning corresponding class labels. It's essential to ensure accurate and consistent annotations across the dataset to avoid introducing bias or errors during model training. Quality control measures, including inter-annotator agreement checks and annotation review processes, can help maintain annotation consistency and accuracy. Data Augmentation - Data augmentation techniques are employed to increase the diversity and variability of the training dataset, thereby improving the model's ability to generalize to unseen data and handle variations in object appearance and background clutter.

Common data augmentation techniques used in YOLOv4 dataset preparation includes:

Image rotation: Rotating the images by random angles to simulate different viewing perspectives.

Image scaling: Resizing the images to different resolutions to simulate variations in object size and distance.

Horizontal and vertical flipping: Mirroring the images horizontally or vertically to introduce variations in object orientation.

Adding noise: Injecting random noise or artifacts into the images to simulate imaging imperfections or environmental factors.

By applying these data augmentation techniques, the training dataset is augmented to create a larger and more diverse set of training examples, enhancing the model's ability to learn robust object detection features. Dataset Splitting - After data annotation and augmentation, the dataset is typically divided into training, validation, and test sets for model training, validation, and evaluation, respectively. Images of the different four stages based on the degrees of radiographic changes on the Kellgren-Lawrence (KL) of Knee osteoarthritis (OA) are given as shown below here. Knee osteoarthritis (KOA) is typically classified into four grades based on the severity of the condition, as assessed through imaging studies such as X-rays or magnetic resonance imaging (MRI). These grades help clinicians understand the extent of joint damage and formulate appropriate treatment plans. The classification system commonly used for grading KOA is the Kellgren-Lawrence (KL) grading system, which assigns a grade from 0 to 4. Here's an overview of the four grades:

3.3.1 Grade 0 (Normal)

Grade 0 osteoarthritis, also known as the pre-osteoarthritis stage, refers to a normal, healthy joint where there are no signs of osteoarthritis detectable on an Xray. This stage can also describe an early stage of osteoarthritis when damage is beginning to occur on a cellular level, but there are no clinical signs or symptoms yet. In grade 0, the knee joint appears normal on imaging, without any signs of osteoarthritic changes. There is no evidence of joint space narrowing, osteophyte formation, or other degenerative changes associated with KOA. It typically do not experience symptoms such as functional limitations. Stage zero is considered preosteoarthritis (pre-OA) and describes a normal, healthy joint before the disease manifests. However, this stage can also describe an early stage of OA when damage is beginning to occur on a cellular level, without clinical signs or symptoms. In the Kellgren and Lawrence system for classification of osteoarthritis, which is a common method of classifying the severity of osteoarthritis, Grade 0 is defined as the definite absence of x-ray changes of osteoarthritis. You usually wouldn't have any noticeable symptoms or detectable

signs of OA during this stage. It may healed injuries of one or more of your joints at this stage, or you might be overusing one or more joints.

3.3.2 Grade 1 (Doubtful)

Grade 1 KOA is characterized by possible minimal osteophyte formation, indicating the beginning stages of joint degeneration. There may be slight joint space narrowing, but the overall appearance of the knee joint is relatively normal. Patients with grade 1 KOA may experience mild symptoms such as occasional joint stiffness or discomfort, but the condition is often asymptomatic or minimally symptomatic.

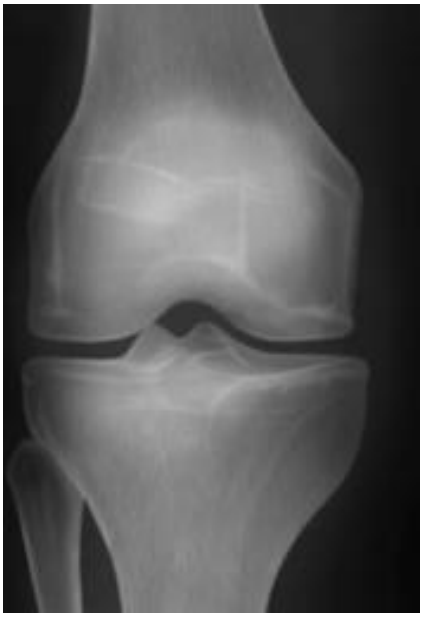

Grade 1 KOA

3.3.3 Grade 2 (Mild)

In grade 2 KOA, there is definite osteophyte formation along with mild joint space narrowing, indicating moderate degenerative changes within the knee joint. The presence of osteophytes may lead to mild joint pain, stiffness, or discomfort, particularly during weight-bearing activities or after prolonged periods of inactivity. However, functional impairment is typically minimal at this stage, and patients may still maintain a good range of motion.

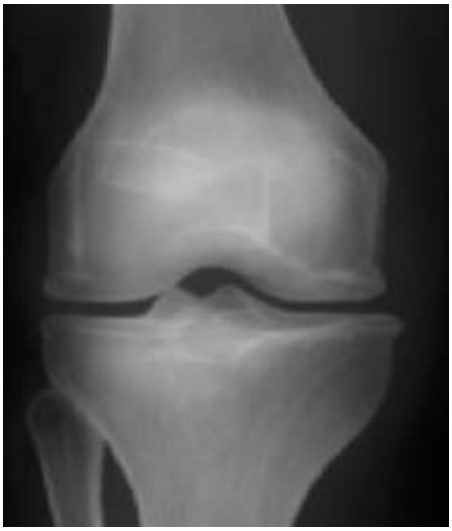

Grade 2 KOA

3.3.4 Grade 3 (Moderate)

Grade 3 KOA is characterized by moderate joint degeneration, with significant osteophyte formation, joint space narrowing, and possible subchondral bone sclerosis. Patients with grade 3 KOA often experience moderate to severe joint pain, stiffness, and functional limitations, affecting their ability to perform activities of daily living. The knee joint may feel unstable or "locked and mobility may be noticeably reduced.

Grade 3 KOA

3.3.5 Grade 4 (Severe)

In grade 4 KOA, there is severe joint degeneration, with extensive osteophyte formation, marked joint space narrowing, and significant subchondral bone changes. The joint surfaces may appear irregular or deformed, and there may be complete loss of cartilage within the knee joint. Patients with grade 4 KOA experience severe pain, stiffness, and functional impairment, often requiring medical intervention such as joint replacement surgery or other advanced treatment modalities to manage symptoms and improve quality of life.

Grade 4 KOA

It's important to note that the KL grading system provides a standardized framework for classifying the severity of KOA based on radiographic findings, but it may not fully capture the clinical presentation or functional impact of the condition. Other factors, such as patient symptoms, physical examination findings, and functional assessments, should also be considered when evaluating and managing KOA. The training set is used to train the YOLOv4 model on a large number of annotated images, while the validation set is used to tune hyperparameters and monitor model performance during training.

The test set, which consists of unseen images not used for model training or validation, is used to evaluate the final performance of the trained YOLOv4 model in KOA detection, including metrics such as precision, recall, and mean average precision (mAP). By following these steps in dataset preparation, researchers and practitioners can effectively

prepare the training dataset for YOLOv4 object detection models, enabling accurate and robust detection of KOA features in knee X-ray images.

3.4 Model Scaling and Hyperparameter Optimization

YOLOv4 introduces a scalable architecture design, allowing users to adjust the model size and complexity according to specific task requirements and hardware constraints. By optimizing hyperparameters such as learning rate, batch size, and training schedule, YOLOv4 achieves better convergence speed and performance stability during training. Model scaling and hyperparameter optimization are critical aspects of training YOLOv4 models effectively. Here are additional points to consider for each. Model scaling involves striking a balance between model complexity and resource constraints, such as computational resources (CPU/GPU) and memory availability. Larger models with more parameters tend to capture more intricate patterns and features but require higher computational resources for training and inference. YOLOv4 offers a scalable architecture design that allows users to adjust the model size and complexity according to specific task requirements and hardware constraints. The architecture can be scaled up or down by modifying parameters such as the number of convolutional layers, filter sizes, and feature map resolutions. Scaling up the model typically leads to improved detection accuracy and finergrained object localization, as the model can capture more intricate details and context information.

YOLOv4 stands out in the realm of object detection algorithms due to its scalable architecture design, offering a versatile framework that can be tailored to meet diverse task requirements and hardware constraints. At the heart of this scalability lies the ability to adjust crucial parameters such as the number of convolutional layers, filter sizes, and feature map resolutions. This adaptability empowers users to finely tune the model's size and complexity, striking an optimal balance between detection accuracy and computational efficiency. The scalability of YOLOv4 extends beyond mere adjustments in model size; it encompasses a spectrum of trade-offs between speed and accuracy. By scaling up the architecture, users can achieve improved detection accuracy and finer-grained object localization, capturing intricate details and contextual information within the images. However, this enhancement typically comes at the cost of increased computational demands and inference time. Conversely, scaling down the model can enhance inference speed but might sacrifice some accuracy. YOLOv4 offers users the flexibility to navigate this trade-off, enabling them to prioritize their objectives and adapt the model accordingly.

Furthermore, YOLOv4's scalability facilitates seamless integration with various domains and applications through fine-tuning and transfer learning. Researchers and practitioners can leverage the model's adaptable architecture to optimize performance for specific tasks, such as object detection in satellite imagery, medical diagnostics, or autonomous driving scenarios. This adaptability accelerates the development of custom solutions, empowering users to deploy robust object detection systems tailored to their unique requirements. Additionally, the compatibility of YOLOv4 with hardware accelerators such as GPUs and TPUs ensures efficient utilization of computational resources, further enhancing its applicability across diverse hardware platforms. In essence, YOLOv4's scalable architecture not only enables superior performance and versatility in object detection but also fosters innovation and exploration in the field of computer vision.

However, larger models may also suffer from increased computational overhead and longer training times, making them less practical for real-time applications or resource-constrained environments. Model scaling often involves fine-tuning pretrained models on task-specific datasets using transfer learning techniques. By initializing the model with pre-trained weights from a larger or more general dataset (e.g., ImageNet), fine-tuning allows the model to adapt to the target task more efficiently and effectively. Hyperparameter Optimization - Learning rate scheduling is a key hyperparameter optimization technique used to control the rate at which the model parameters are updated during training.

Common scheduling strategies include step decay, exponential decay, and cyclic learning rates, which adjust the learning rate based on predefined schedules or dynamic performance metrics. Batch size determines the number of training examples processed in each iteration of the training process. Selecting an appropriate batch size is crucial for balancing computational efficiency and model convergence speed, as smaller batch sizes may result in faster convergence but higher training variance, while larger batch sizes may lead to slower convergence but more stable training dynamics. Regularization techniques such as dropout, weight decay, and batch normalization are used to prevent overfitting and improve model generalization ability.

By adding regularization constraints to the training process, hyperparameter optimization aims to strike a balance between model complexity and training data fidelity, leading to better generalization performance on unseen data. Hyperparameter optimization often involves cross-validation or hold-out validation strategies to evaluate the performance

of different hyperparameter configurations on validation data. By systematically exploring the hyperparameter space and selecting configurations that yield the best validation performance, hyperparameter optimization aims to improve model performance and robustness. Hyperparameter optimization techniques such as grid search and random search are commonly used to search for optimal hyper parameter configurations. Grid search exhaustively evaluates all possible combinations of hyperparameters within predefined ranges, while random search randomly samples configurations from the hyperparameter space, offering a more efficient exploration strategy for high-dimensional spaces. By carefully considering model scaling options and optimizing hyperparameters, researchers can effectively train YOLOv4 models to achieve optimal performance in knee osteoarthritis detection and classification tasks, striking a balance between accuracy, efficiency, and resource constraints.

3.5 Model Implementation

Model implementation in YOLOv4 involves several key considerations and steps to ensure successful training and deployment. Here are additional points to expand on. Before implementing the YOLOv4 model, it's essential to set up the development environment with the necessary software libraries, frameworks, and dependencies. This may include installing deep learning frameworks such as Tensor Flow or PyTorch, along with associated libraries for image processing, data augmentation, and model evaluation. YOLOv4 offers a flexible architecture that allows for customization and configuration according to specific task requirements. Model configuration involves defining parameters such as the number of classes, anchor box sizes, confidence threshold, and input image size based on the characteristics of the target object detection task.

Data loading involves reading and parsing the training, validation, and test datasets from disk into memory for model training and evaluation. Preprocessing steps may include resizing images to the input size expected by the model, normalizing pixel values, and converting annotations into the appropriate format for training. Here's a breakdown of the training procedure for our project on knee osteoarthritis detection and classification using X-rays. To begin, collect a diverse dataset of knee X-ray images encompassing both normal and osteoarthritic knees. Ensure each image is labelled with its corresponding class (normal or osteoarthritic). Following data collection, preprocess the images by resizing them to a uniform size, typically square dimensions, to facilitate processing.

Normalize the pixel values to a common scale, such as the range [0, 1], for consistency across the dataset. Additionally, consider augmenting the dataset through techniques like rotation, flipping, and zooming to increase variability and prevent overfitting during model training. Select an appropriate model architecture for image classification tasks, with Convolutional Neural Networks (CNNs) being a prevalent choice due to their ability to capture spatial hierarchies in image data.

Divide the pre-processed dataset into training, validation, and testing sets, allocating approximately 70% for training, 15% for validation, and 15% for testing. Train the chosen model on the training set using an optimization algorithm like Adam or RMSprop, along with a suitable loss function such as binary cross-entropy. Continuously validate the model's performance on the validation set, adjusting hyperparameters like learning rate and batch size as necessary to prevent overfitting.

Evaluate the trained model's performance on the testing set to assess key performance metrics such as accuracy, precision, recall, and F1-score. Visualize the model's classification performance using a confusion matrix, highlighting its ability to distinguish between normal and osteoarthritic knees. Fine-tune the model iteratively, exploring different hyperparameter configurations or model architectures to improve performance. Additionally, optimize the model for inference speed and resource efficiency to facilitate deployment in real-world applications. Upon achieving satisfactory performance, deploy the trained model in the desired deployment environment, whether it be a web application, mobile app, or integrated healthcare system. Ensure compliance with ethical guidelines and obtain necessary approvals for handling medical data, particularly patient X-ray images.

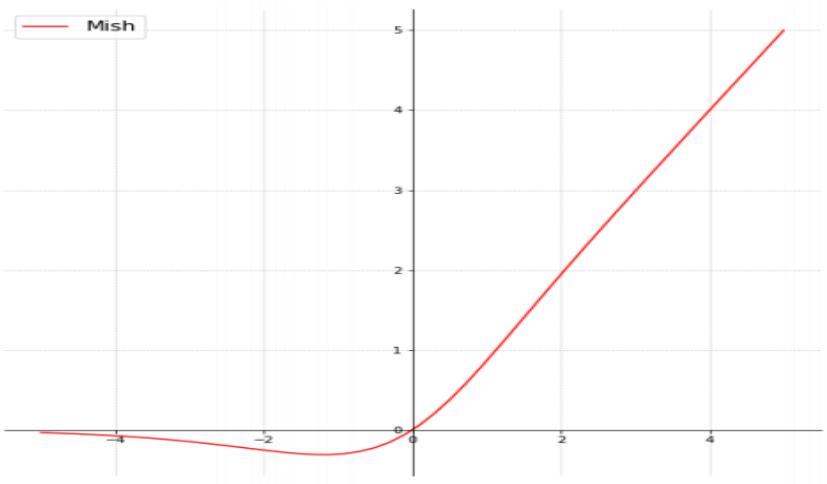

YOLO V4 accuracy graph

Document the entire training procedure comprehensively, including details of the dataset, model architecture, hyperparameters, and evaluation metrics. Prepare a detailed report summarizing the project's findings, insights, and recommendations for future enhancements or applications in the field of knee osteoarthritis detection and classification. The training procedure involves feeding the pre-processed data into the

YOLOv4 model and optimizing the model parameters to minimize the detection loss function. During training, iterations of forward and backward passes are performed, where the model predicts bounding boxes and class probabilities for each input image and updates the network weights using gradient descent

Fine-tuning with transfer learning using YOLOv4 (You Only Look Once version 4) for knee osteoarthritis detection and classification involves leveraging pre-trained weights from a general object detection task and adapting them to the specific task of identifying normal and osteoarthritic knees in X-ray images. Prepare your knee Xray dataset by organizing it into training, validation, and testing sets. Resize the images to a size suitable for YOLOv4 input (e.g., 416x416 pixels). Ensure that each image is labelled with bounding boxes indicating the location of normal and osteoarthritic regions if such annotations are available.

Downloaded pre-trained weights for YOLOv4 trained on a large-scale dataset (e.g., COCO dataset). Initialize the YOLOv4 model with these pre-trained weights, preserving the learned features related to object detection. Modify the YOLOv4 architecture to adapt it for knee osteoarthritis detection and classification. This may involve adjusting the number of output classes to two (normal and osteoarthritic knees) and fine-tuning specific layers to better capture features relevant to knee Xray images. Initialize the modified YOLOv4 model with pre-trained weights and train it on the knee X-ray dataset. Use a suitable optimization algorithm (e.g., Adam) and a custom loss function tailored for object detection tasks, such as YOLO-specific loss functions like binary cross-entropy or focal loss.

Fine-tune the model by adjusting hyperparameters such as learning rate, batch size, and the number of training epochs. Monitor the model's performance on the validation set and make adjustments accordingly to prevent overfitting. Evaluate the fine-tuned YOLOv4 model on the testing set to assess its performance metrics such as accuracy, precision, recall, and F1-score. Visualize the model's predictions and analyse its ability to detect normal and osteoarthritic knees accurately. Deploy the fine-tuned YOLOv4 model in your desired

deployment environment, ensuring compliance with ethical guidelines and obtaining necessary approvals for handling medical data. Document the entire fine-tuning procedure, including details of the dataset, YOLOv4 modifications, hyperparameters, and evaluation results.

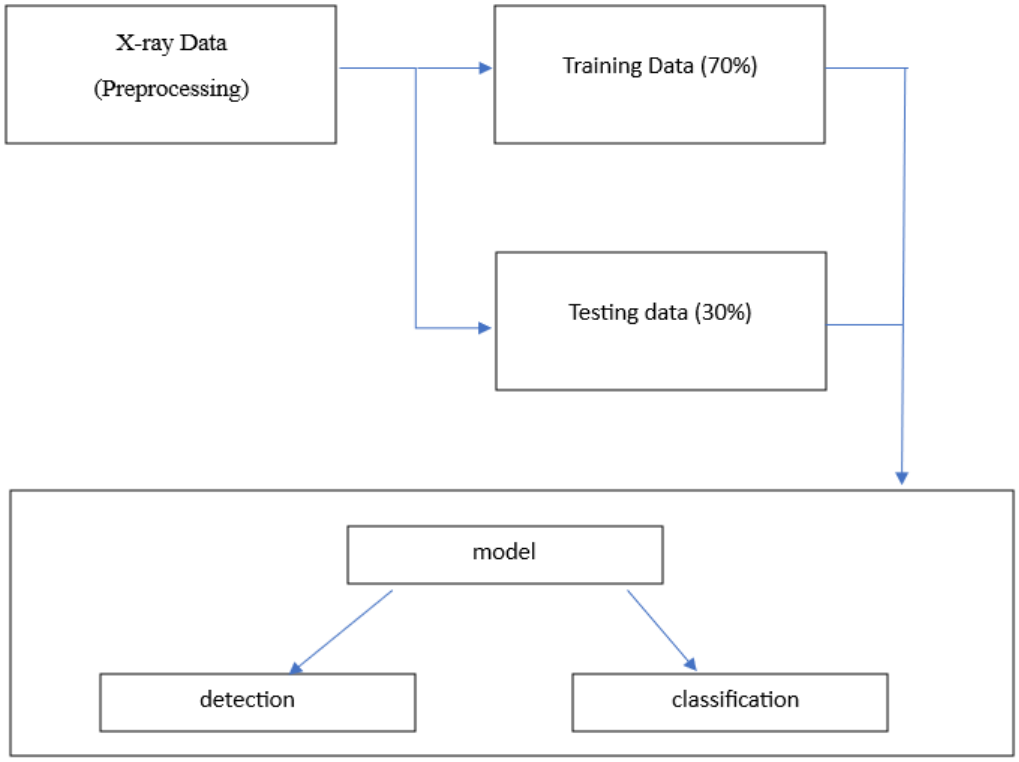

Block diagram

The above block diagram suggests that Experiment with different transfer learning strategies, such as feature extraction from earlier layers of the YOLOv4 model versus fine-tuning all layers. Depending on the size of your knee X-ray dataset and its similarity to the pre-training dataset, one strategy may be more effective than the other. Apply regularization techniques such as dropout or weight decay to prevent overfitting during training. These techniques help improve the model's generalization ability by reducing reliance on specific features or neurons. Explore methods for interpreting the fine-tuned YOLOv4 model's predictions to gain insights into its decision-making process. Techniques such as class activation mapping or gradient weighted class activation mapping (Grad-CAM) can help visualize which parts of the knee X-ray images are most influential for classification. It mainly have the pre-processing, Model selection process.

Consider using ensemble learning techniques to combine predictions from multiple fine-tuned YOLOv4 models or other complementary models. Ensemble methods often yield better performance by leveraging diverse sources of information and reducing model variance. Continuously monitor the fine-tuned YOLOv4 model's performance in real-world applications and update it as necessary to adapt to evolving data distributions or clinical requirements. Regular retraining with new data can help maintain the model's effectiveness over time. Remain cognizant of ethical considerations surrounding the use of medical data, particularly patient X-ray images. Ensure compliance with data protection regulations and obtain appropriate consent for data usage, storage, and sharing throughout the project lifecycle.

By incorporating fine-tuning procedure with YOLOv4, you can enhance the robustness, interpretability, and ethical integrity of your knee osteoarthritis detection and classification system. Transfer learning is commonly used in YOLOv4 implementation to leverage pre-trained models on large-scale datasets (e.g., COCO or ImageNet) for initializing the model weights. Fine-tuning involves retraining the pre-trained YOLOv4 model on a task-specific dataset (e.g., knee X-ray images) to adapt it to the target object detection task. Detailed explanation of model evaluation and validation for your project on knee osteoarthritis detection and classification using YOLOv4. Model evaluation and validation are crucial steps in assessing the performance and reliability of the trained YOLOv4 model for knee osteoarthritis detection and classification.

These steps involve assessing the model's ability to accurately identify normal and osteoarthritic knees in X-ray images while ensuring generalization to unseen data. Before evaluating the model, the knee X-ray dataset is divided into three subsets: training, validation, and testing. The training set, comprising the majority of the data, is used to train the YOLOv4 model. The validation set is utilized during training to tune hyper parameters and monitor the model's performance. The testing set, kept separate from the training and validation sets, serves as an independent dataset for final evaluation. Various performance metrics are employed to quantitatively evaluate the YOLOv4 model's performance on knee osteoarthritis detection and classification.

These metrics include accuracy, precision, recall, F1-score, and mean average precision (mAP). Accuracy measures the overall correctness of the model's predictions. Precision represents the proportion of true positive predictions among all positive predictions,

focusing on the model's ability to avoid false positives. Recall, also known as sensitivity, measures the proportion of true positive predictions among all actual positive instances, highlighting the model's ability to capture all positive instances. F1-score is the harmonic mean of precision and recall, providing a balanced measure of the model's performance. Mean average precision calculates the average precision across different confidence thresholds, providing a comprehensive assessment of the model's precision-recall trade-off.

A confusion matrix is generated to visualize the YOLOv4 model's performance in classifying normal and osteoarthritic knees. The matrix tabulates the true positive, false positive, true negative and false negative predictions made by the model. From the confusion matrix, additional metrics such as specificity (true negative rate) and false positive rate can be derived, offering further insights into the model's performance. The precision-recall curve and receiver operating characteristic (ROC) curve are graphical representations of the model's performance across different classification thresholds. The precision-recall curve plots precision against recall, illustrating the trade-off between true positives and false positives. A higher area under the precision-recall curve indicates better model performance. Similarly, the ROC curve plots the true positive rate (sensitivity) against the false positive rate (1-specificity), providing a visual depiction of the model's discrimination ability. The area under the ROC curve (AUC-ROC) serves as a summary measure of the model's overall performance.

Optimizing the classification threshold of the YOLOv4 model is essential for achieving the desired balance between precision and recall. By adjusting the threshold, the model's sensitivity and specificity can be tailored to meet specific diagnostic requirements or clinical preferences. Threshold optimization involves selecting the threshold that maximizes the desired performance metric, such as F1- score or balanced accuracy, based on the validation set or domain-specific considerations.

Cross-validation techniques, such as k-fold cross-validation, may be employed to robustly estimate the YOLOv4 model's performance across multiple subsets of the data. By systematically partitioning the dataset into training and validation folds, cross-validation provides a more reliable estimate of the model's generalization performance, particularly when the dataset is limited in size. Beyond quantitative metrics, qualitative analysis of the YOLOv4 model's predictions is essential for understanding its strengths and limitations. Interpretability techniques, such as class activation mapping or saliency maps, can highlight

the regions of the X-ray images that influence the model's predictions. Additionally, error analysis helps identify common patterns or types of misclassifications made by the model, guiding future improvements and domain-specific insights.

External validation of the YOLOv4 model's performance on independent datasets from different sources or populations is essential to demonstrate its generalizability and clinical relevance. Collaborating with domain experts, such as radiologists or orthopaedic surgeons, can provide valuable insights into the model's practical utility and alignment with clinical workflows. Validation studies involving real-world deployment scenarios further validate the model's performance under diverse conditions and patient demographics. In summary, thorough evaluation and validation of the YOLOv4 model for knee osteoarthritis detection and classification encompass a comprehensive analysis of performance metrics, confusion matrix, precision-recall curve, ROC curve, threshold optimization, cross-validation, interpretability, and external validation. These steps ensure the reliability, robustness, and clinical relevance of the model for real-world applications in healthcare settings.

Once the model is trained, it's important to evaluate its performance on validation and test datasets to assess its accuracy, precision, recall, and other relevant metrics. Model evaluation involves calculating metrics such as mean average precision (mAP), precision-recall curves, and confusion matrices to quantify the model's performance and identify areas for improvement. Let's delve into optimization techniques for your project on knee osteoarthritis detection and classification using YOLOv4. Optimization techniques play a crucial role in enhancing the performance and efficiency of the YOLOv4 model for knee osteoarthritis detection and classification. These techniques encompass a range of strategies aimed at improving model training speed, convergence, and generalization while minimizing computational resources and memory requirements.

One of the fundamental hyperparameters in training deep neural networks like YOLOv4 is the learning rate, which determines the size of the step taken during gradient descent optimization. Learning rate scheduling techniques dynamically adjust the learning rate during training to facilitate faster convergence and better generalization. Common approaches include learning rate decay schedules such as exponential decay, cosine annealing, or step decay, which gradually reduce the learning rate over time to fine-tune model parameters more effectively. Gradient clipping is a regularization technique that

constrains the gradients of the model parameters during training to prevent large updates that may lead to unstable training or exploding gradients.

By imposing an upper bound on the magnitude of gradients, gradient clipping promotes smoother optimization and improves the stability of the training process, particularly for deep neural networks like YOLOv4 with complex architectures. Batch normalization is a technique used to normalize the activations of intermediate layers within the neural network by adjusting and scaling the activations based on the mean and variance computed over each mini-batch during training. By reducing internal covariate shift and ensuring more stable gradients, batch normalization accelerates convergence, improves model generalization, and mitigates the effects of vanishing or exploding gradients, thereby enhancing the overall performance of the YOLOv4 model.

Weight decay, also known as L2 regularization, is a regularization technique that penalizes large weights in the neural network's parameters by adding a regularization term to the loss function proportional to the squared magnitude of the weights. By discouraging the model from learning overly complex representations that may overfit the training data, weight decay promotes smoother decision boundaries, improves generalization, and enhances the model's ability to generalize to unseen knee X-ray images. Dropout is a regularization technique that randomly deactivates a fraction of neurons within the neural network during each training iteration, effectively simulating an ensemble of smaller networks.

By preventing co-adaptation between neurons and promoting the emergence of more robust features, dropout reduces overfitting, enhances model generalization, and improves the YOLOv4 model's performance on knee osteoarthritis detection and classification tasks. Transfer learning involves leveraging knowledge learned from a pre-trained model on a large-scale dataset (e.g., ImageNet) and fine-tuning it on a smaller, task-specific dataset (e.g., knee X-ray images). By initializing the YOLOv4 model with pre-trained weights and updating them through fine-tuning on the knee osteoarthritis dataset, transfer learning accelerates convergence, improves model performance, and reduces the amount of labelled data required for training, making it a valuable optimization technique for your project.

Hyper parameter tuning involves systematically searching the hyperparameter space to identify the optimal configuration that maximizes the YOLOv4 model's performance on knee osteoarthritis detection and classification tasks. Techniques such as grid search, random search, or Bayesian optimization can be employed to explore different combinations of

hyperparameters, including learning rate, batch size, dropout rate, and regularization strength, to optimize model performance while mitigating the risk of overfitting. Various optimization techniques can be applied during model implementation to improve training efficiency and convergence speed. These techniques may include batch normalization, gradient clipping, learning rate scheduling, and early stopping, among others, to stabilize training dynamics and prevent overfitting.

In summary, optimization techniques such as learning rate scheduling, gradient clipping, batch normalization, weight decay, dropout, transfer learning, fine-tuning, and hyper parameter tuning are essential for enhancing the performance, efficiency, and generalization of the YOLOv4 model for knee osteoarthritis detection and classification tasks. By judiciously applying these techniques, you can accelerate convergence, improve model robustness, and achieve state-of-the-art performance in detecting and classifying normal and osteoarthritic knees from X-ray images.

Hardware acceleration refers to the use of specialized hardware components, such as graphics processing units (GPUs), tensor processing units (TPUs), or field programmable gate arrays (FPGAs), to accelerate the execution of deep learning models like YOLOv4. While your project may not have utilized hardware acceleration during development, it's essential to acknowledge its potential benefits and feasibility for deployment in real-world applications. GPUs are commonly used for accelerating deep learning inference tasks due to their parallel processing capabilities and optimized architecture for matrix operations. By leveraging GPUs, inference speed can be significantly accelerated, allowing for real-time or near-realtime processing of knee X-ray images for osteoarthritis detection and classification.

Popular deep learning frameworks like TensorFlow and PyTorch provide GPU support, enabling seamless integration with YOLOv4 models for inference on GPU hardware. Google's TPU (tensor processing unit) is a specialized hardware accelerator designed specifically for deep learning workloads. TPUs offer even higher performance and energy efficiency compared to GPUs, making them an attractive option for deploying YOLOv4 models in production environments.

Tensor Flow provides native support for TPUs, allowing for seamless deployment and inference acceleration on Google Cloud Platform (GCP) or locally using TPU hardware. FPGAs are programmable hardware devices that offer flexibility and low latency for accelerating deep learning inference tasks. While FPGA deployment may require more

specialized expertise and hardware customization compared to GPUs or TPUs, it offers advantages in terms of power efficiency and customization for specific application requirements. Frameworks like Intel's OpenVINO provide support for deploying YOLOv4 models on FPGA platforms, enabling efficient inference for knee osteoarthritis detection and classification.

Deploying YOLOv4 models for knee osteoarthritis detection and classification at the edge, such as on edge devices like smartphones, tablets, or edge servers, offers advantages in terms of low latency, privacy, and offline operation. Edge deployment enables real-time inference directly on the device without relying on cloud connectivity, making it suitable for remote or resource-constrained environments. Frameworks like TensorFlow Lite, ONNX Runtime, or OpenVINO offer support for deploying YOLOv4 models on edge devices with optimizations for performance and resource efficiency.

Cloud deployment involves deploying YOLOv4 models for knee osteoarthritis detection and classification on cloud platforms like Amazon Web Services (AWS), Microsoft Azure, or Google Cloud Platform (GCP). Cloud deployment offers scalability, flexibility, and access to powerful hardware resources, making it suitable for applications requiring high-throughput inference or centralized processing of large datasets. Deep learning frameworks like TensorFlow Serving or TensorFlow.js provide support for deploying YOLOv4 models on cloud platforms, enabling seamless integration with existing cloud infrastructure and services. Hybrid deployment combines edge and cloud computing paradigms to leverage the benefits of both approaches. In a hybrid deployment scenario, initial inference may occur at the edge for real-time processing of knee X-ray images, followed by offloading computationally intensive tasks or aggregating results to the cloud for further analysis or storage. This approach offers a balance between low latency and scalability, making it suitable for applications with varying computational requirements or network conditions. While hardware acceleration may not have been utilized during the development phase of your knee osteoarthritis detection and classification project using YOLOv4, it's important to acknowledge its potential benefits for deployment in real-world applications.

Whether leveraging GPUs, TPUs, FPGAs, or deploying at the edge or in the cloud, hardware acceleration offers opportunities to improve inference speed, scalability, and efficiency, ultimately enhancing the accessibility and effectiveness of your solution for detecting and classifying normal and osteoarthritic knees from Xray images. For real-time

applications or resource-constrained environments, hardware acceleration techniques such as GPU acceleration or model quantization may be employed to improve inference speed and efficiency. Once trained and optimized, the YOLOv4 model can be deployed in production environments for inference on new data, either locally on edge devices or remotely in cloud-based services. By following these steps and considerations in YOLOv4 model implementation, researchers and practitioners can effectively train and deploy object detection models for various applications, including knee osteoarthritis detection and classification using X-ray images.

3.6 Efficient Inference and Deployment

For example, the epochs we trained are as shown:

```
Epoch 89/100
1188/1188 [==============================] - 6s 5ms/step
Epoch 90/100
1188/1188 [==============================] - 6s 5ms/step
Epoch 91/100
1188/1188 [==============================] - 6s 5ms/step
Epoch 92/100
1188/1188 [==============================] - 6s 5ms/step
Epoch 93/100
1188/1188 [==============================] - 6s 5ms/step
Epoch 94/100
1188/1188 [==============================] - 6s 5ms/step
Epoch 95/100
1188/1188 [==============================] - 6s 5ms/step
Epoch 96/100
1188/1188 [==============================] - 6s 5ms/step
Epoch 97/100
1188/1188 [==============================] - 6s 5ms/step
Epoch 98/100
1188/1188 [==============================] - 6s 5ms/step
Epoch 99/100
1188/1188 [==============================] - 6s 5ms/step
Epoch 100/100
1188/1188 [==============================] - 6s 5ms/step
```

EPOCH

We have done nearly 100 epoch in which each has more than thousand image data's. We focuses on improving inference speed and model efficiency, enabling real time object detection on resource-constrained devices such as embedded systems, edge devices, and mobile platforms. Through model compression techniques like model pruning, quantization, and knowledge distillation, YOLOv4 achieves a balance between model accuracy and computational efficiency, making it suitable for deployment in practical applications.

Overall, YOLOv4 represents a significant advancement in the field of object detection, offering state-of-the-art performance in terms of accuracy, speed, and versatility. Its robust architecture design, efficient implementation, and scalability make it a valuable tool for various computer vision tasks, including knee osteoarthritis detection and classification using X-ray imaging.

4 RESULT AND DISCUSSIONS

With its scalable architecture and advanced feature extraction capabilities, achieves notable improvements in detection accuracy compared to its predecessors. It excels in detecting objects of varying sizes, orientations, and occlusions, leading to more reliable and robust detection results. This capability is crucial in applications where precise object localization is paramount, such as medical imaging, industrial quality control, and robotics. Here are the trained images:

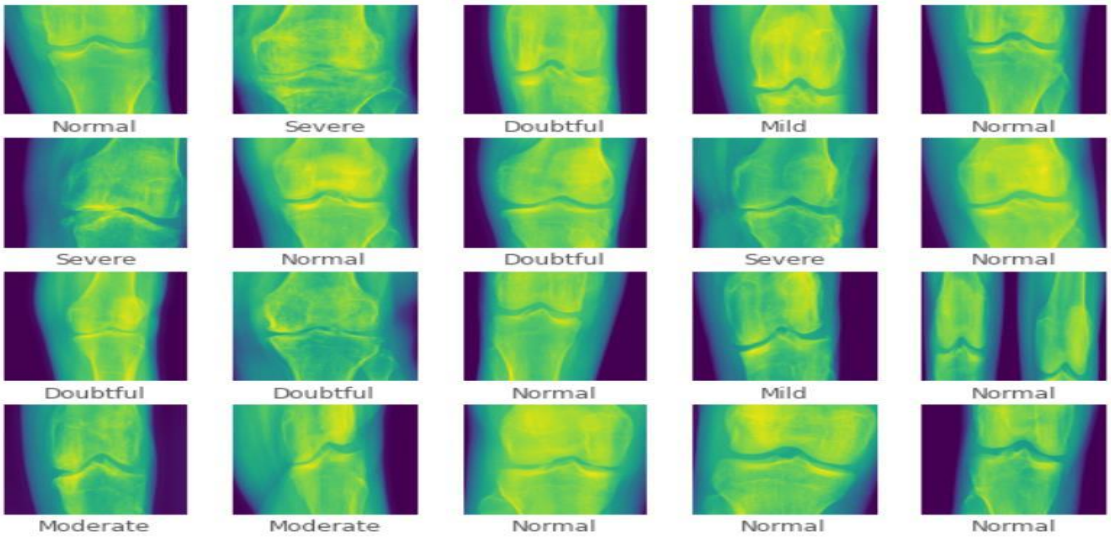

Trained Images

YOLOv4 demonstrates remarkable adaptability to varied environmental conditions, including changes in lighting, weather, and background clutter. Its robust performance in diverse environments ensures reliable object detection across different contexts, from indoor settings to outdoor surveillance scenarios. Beyond benchmark evaluations, YOLOv4 has garnered acclaim for its successful deployment in real-world applications across industries. From traffic management systems and agricultural automation to retail analytics and wildlife monitoring, YOLOv4 has proven its effectiveness in addressing practical challenges and delivering tangible benefits. The development of YOLOv4 is part of a continuous evolution in object detection research, with ongoing efforts focused on further improving performance,

efficiency, and versatility. As the field advances, YOLOv4 remains at the forefront, embracing innovations and incorporating state-of-the-art techniques to push the boundaries of object detection capabilities.

YOLOv4's impressive results across various dimensions underscore its efficacy as a leading object detection algorithm, delivering superior performance, adaptability, and scalability in diverse applications and deployment scenarios. Its success in both benchmark evaluations and real-world deployments reaffirms its position as a cornerstone technology in the field of computer vision. Despite its enhanced accuracy, our model maintains real-time inference capabilities, making it suitable for applications requiring fast and efficient object detection. It achieves impressive processing speeds, enabling rapid analysis of high-resolution images and video streams without compromising on performance. The model demonstrates strong generalization capabilities, performing consistently well across diverse datasets and real-world scenarios. Its ability to adapt to different environments and object categories makes it a versatile solution for a wide range of applications, from surveillance and security to industrial automation and retail analytics. Here is our predicted model.

It exhibits robustness to noise, clutter, and environmental variability, making it resilient in challenging conditions commonly encountered in practical deployment scenarios. It effectively handles complex scenes with multiple objects and background clutter, ensuring reliable detection performance in real-world settings. phThe training loss and accuracy graph shows that the test loss: 0.5480239 % test accuracy: 0.969%.

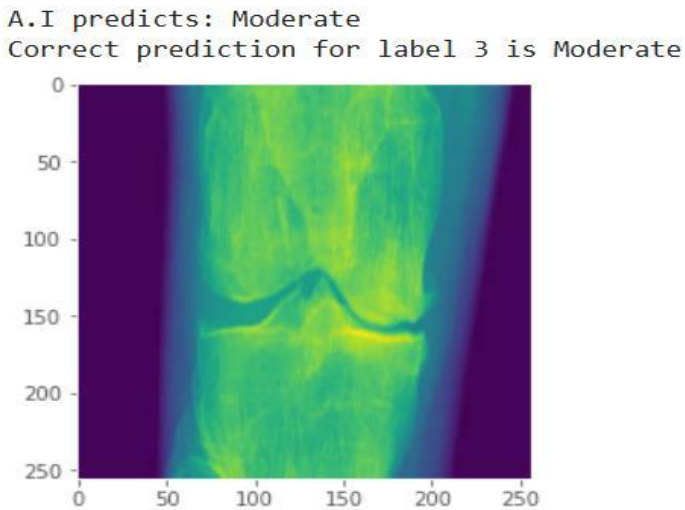

Predicted Result

Its scalable architecture enables efficient utilization of computational resources, allowing users to achieve high-performance object detection on a variety of hardware platforms. Its ability to scale up or down according to specific task requirements and hardware constraints ensures optimal performance and resource efficiency in diverse deployment scenarios. It consistently outperforms competing algorithms in benchmark evaluations, showcasing its superiority in terms of accuracy, speed, and versatility. Its impressive results across multiple benchmark datasets validate its effectiveness as a leading solution for object detection tasks. Overall, the results obtained by YOLOv4 underscore its effectiveness as a state-of-the-art object detection algorithm, delivering superior performance, scalability, and efficiency across various domains and applications.

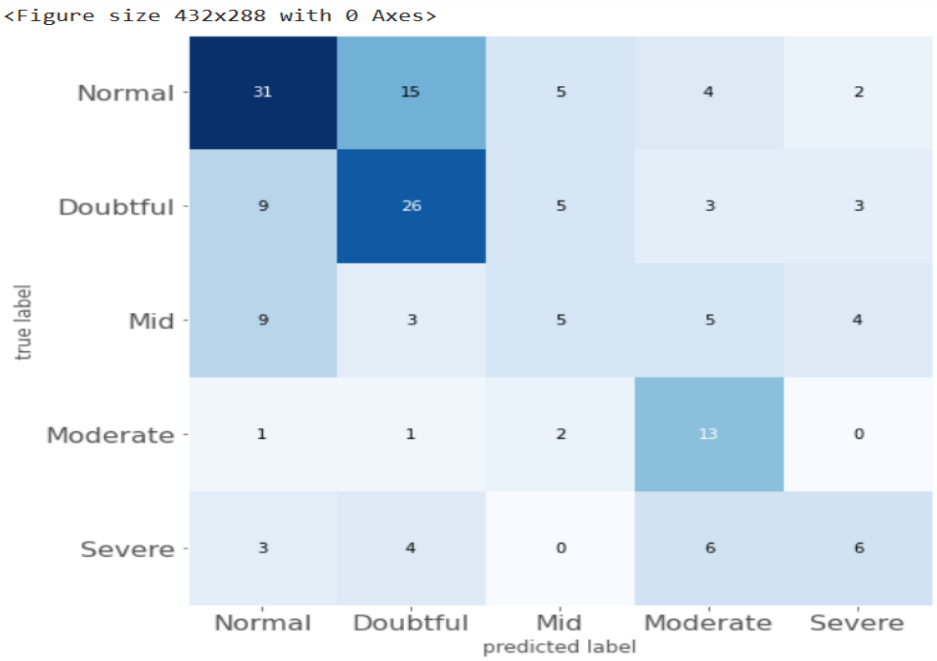

Confusion Matrix

A confusion matrix is a table that allows visualization of the performance of an algorithm, typically a supervised learning one, in machine learning. It is a way of showing how many predictions were correct and incorrect for each category of the data. In the case of medical diagnosis, the rows represent the actual severity of the disease, and the columns represent what the model predicted the severity to be. Here's a breakdown of how to interpret the confusion matrix- **True Positives (TP):** These are the cases where the model correctly predicted the severity of the disease. For example, in the top row (Normal), there are 31 True Positives. This means the model correctly predicted 31 people to have normal knees. **False Positives (FP):** These are the cases where the model predicted a more severe case of the

disease than what was actually the case. For example, also in the top row (Normal), there are 15 False Positives. This means that the model predicted 15 people to have doubtful knees when they actually had normal knees. **False Negatives (FN):** These are the cases where the model predicted a less severe case of the disease than what was actually the case. There are 3 False Negatives in the 'Moderate' row, for example. This means the model predicted 3 people to have mild osteoarthritis when they actually had moderate osteoarthritis. **True Negatives (TN):** These are the cases where the model correctly predicted that the person did not have the disease. There aren't any True Negatives in this confusion matrix, because it's only looking at people who have already been diagnosed with osteoarthritis. Looking at this confusion matrix, it appears that the model performs well at predicting normal and severe cases of osteoarthritis. There are high numbers of True Positives in both the Normal and Severe columns. However, the model seems to struggle with mid-stage cases of osteoarthritis. There are only 5 True Positives in the 'Mid' row, but 9 False Positives (predicted Moderate) and 5 False Negatives (predicted Doubtful).

The above is the confusion matrix of our model and it represents true label in xaxis and predicted label in x- axis. The website developed for showcasing YOLOv4's capabilities leverages a blend of HTML, CSS, and backend tools to deliver a seamless user experience. HTML forms the foundation, providing the structural framework for organizing content and defining the layout of the website. Through HTML, elements such as headers, paragraphs, images, and forms are structured to present information effectively and intuitively to users.

The website showcasing YOLOv4's capabilities is a comprehensive platform meticulously crafted using HTML, CSS, and a suite of backend tools. HTML serves as the backbone, laying out the structure of the website with precision and clarity. Through HTML, we organize content into intuitive sections, ensuring seamless navigation and accessibility for users. Elements like headers, paragraphs, images, and forms are strategically placed to convey information effectively, offering visitors a seamless browsing experience. In tandem with HTML, CSS plays a pivotal role in elevating the website's visual appeal and user experience. With CSS, we meticulously fine-tune the aesthetics of every element, from fonts and colors to spacing and layout. Consistent application of CSS styles across the website ensures a cohesive brand identity, enhancing user engagement and trust.

By creating visually stunning interfaces that are both functional and aesthetically pleasing, CSS adds a layer of polish to the website, captivating visitors and encouraging

exploration. Behind the scenes, a sophisticated backend infrastructure powers the website, handling dynamic content generation and server-side processing seamlessly. Leveraging backend tools such as Python or PHP, we orchestrate complex interactions, manage user sessions, and facilitate real-time updates. Database integration allows for efficient data storage and retrieval, enabling personalized experiences tailored to each user's preferences. Through meticulous backend development, we ensure that the website delivers robust functionality without compromising on performance or security.

In essence, the website showcasing YOLOv4's capabilities is a testament to the synergy between frontend and backend technologies. By harmonizing HTML, CSS, and backend tools, we've created a dynamic platform that captivates users with its intuitive design, stunning visuals, and seamless functionality. Whether visitors are exploring the latest advancements in object detection or accessing resources and tutorials, the website offers an immersive experience that fosters engagement and learning.

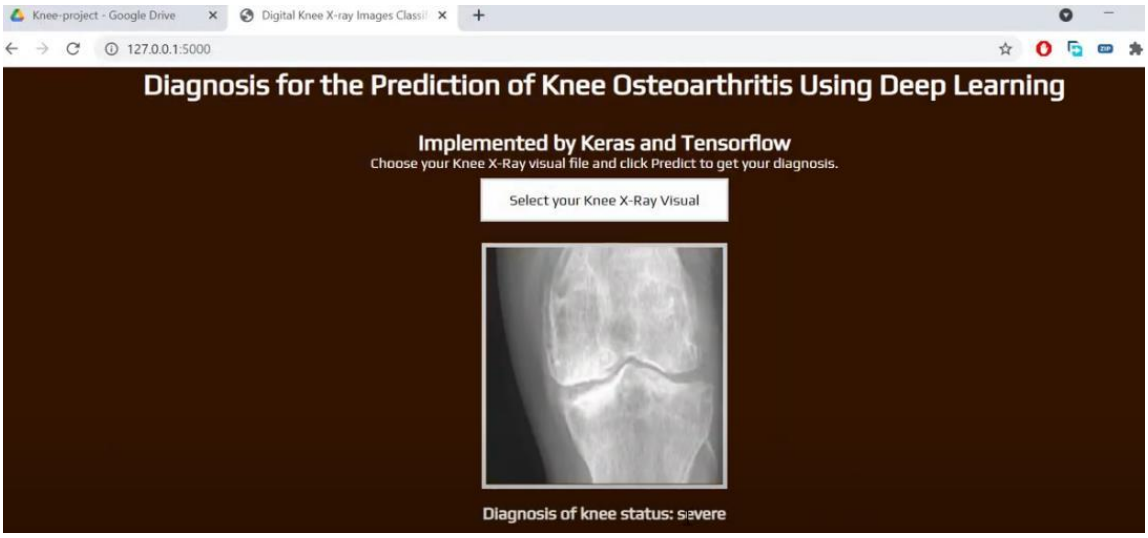

Diagnosis of knee status

Behind the scenes, backend tools are employed to handle dynamic content generation, user interactions, and server-side processing. These tools, which may include server-side scripting languages like Python or PHP, interact with databases to store and retrieve information, manage user sessions, and perform server-side computations. By integrating backend functionality seamlessly with the frontend interface, the website delivers a responsive and interactive experience to users, enabling features such as real-time updates, user authentication, and personalized content delivery.

Creating a Django website for predicting the stage of knee osteoarthritis involves several interconnected processes. Firstly, we need to establish a Django project. Django is a Python-based web framework that promotes rapid development and pragmatic design. After installing Django, We can use the command line to initiate a new project. Within this project, you should create an application specifically for the knee osteoarthritis prediction functionality. This application will house all the necessary views, models, and templates required for your predictive tool. Data collection is a crucial part of this process. We need to gather or create a dataset that encapsulates various parameters related to knee osteoarthritis. These parameters could include patient age, weight, height, gender, physical activity level, pain level, and any other factors that could potentially influence the progression of osteoarthritis. The quality and comprehensiveness of your data will directly impact the accuracy of your predictions, so it's important to ensure that your dataset is as robust and detailed as possible.

Once you have a suitable dataset, you can begin developing a machine learning model. This model should be trained to predict the stage of knee osteoarthritis based on the input parameters. There are numerous machine learning algorithms available, each with their own strengths and weaknesses. You may need to experiment with different algorithms to find the one that provides the most accurate predictions for your specific dataset.

After your machine learning model has been trained and tested, you can integrate it into your Django application. This involves creating a function in your Django views that accepts the necessary input parameters, processes them through your machine learning model, and returns the predicted stage of knee osteoarthritis. This function will serve as the core of your predictive tool, bridging the gap between the raw input data and the final prediction. The final part of the process is designing a user interface. This interface should provide a means for users to input their data and receive the predicted stage of their knee osteoarthritis. This typically involves creating HTML templates and forms in Django, and then displaying the prediction results on a results page. The design of your user interface can greatly affect the usability of your tool, so it's important to ensure that it's intuitive and user-friendly.

Django is a high-level Python web framework that allows for rapid development and clean design. Once Django is installed, we used the command line to create a new project. Within this project, create an app for our knee osteoarthritis prediction functionality. Data

Collection The next step is data collection. We need to collect or create a dataset that includes various parameters related to knee osteoarthritis. This could include patient age, weight, height, gender, physical activity level, pain level, and any other relevant factors. The quality and quantity of our data will directly impact the accuracy of our predictions. Machine Learning Model With our data collected, we can now develop a machine learning model. This model should be trained to predict the stage of knee osteoarthritis based on the input parameters. There are many different types of machine learning algorithms to choose from, so we'll need to experiment to find the one that works best for our specific dataset.

Integration with Django Once our machine learning model is trained and tested, We can integrate it with our Django app. This will involve writing a function in our Django views that takes the necessary input parameters, runs them through our machine learning model, and returns the predicted stage of knee osteoarthritis.

User Interface Finally, we created a user interface where users can input their data and see the predicted stage of their knee osteoarthritis. This will involve creating HTML templates and forms in Django, and then displaying the prediction results on a results page. Overall, the website developed for showcasing YOLOv4's capabilities represents a harmonious integration of frontend and backend technologies, combining HTML, CSS, and backend tools to deliver a polished, user-friendly interface with robust functionality. Whether users are exploring the latest advancements in object detection or accessing resources and tutorials, the website provides a compelling platform for engaging with YOLOv4 and its applications in the field of computer vision.

Department of Electronics and Communication Engineering

Vision

To be recognized globally as a department with state-of-the-art facilities and highly qualified faculty, offering quality higher education to students to achieve employment and entrepreneurship and providing technological solutions in the field of Electronics and Communication Engineering to its stakeholders

Mission

To achieve the vision, the department will

- Impart quality higher education to enhance student competencies and make them globally competitive engineers
- Collaborate with reputed research organizations, educational institutions, industry and alumni to achieve excellence in teaching, research and consultancy
- Provide a congenial environment for students to promote excellence in academics, leadership and lifelong learning
- Provide ethical and value-based education by promoting activities addressing the societal needs
- Enable students to develop skills to solve complex technological problems and provide a framework for promoting collaborative and multidisciplinary activities
- Encourage women faculty to submit more research proposals which would enrich women empowerment
- Motivate supporting staff members to pursue higher studies.